Icing in SLD (Supercooled Large Droplet), ICI (Ice Crystal Icing) and snow conditions

B. Aguilar[2], T. Alary[2], L. Bennani[2], P. Berthoumieu[2], G. Blanchard[2], V. Bodoc[2], M. Bouyges, B. Dejean[2], Q. Duchayne[2], C. Laurent[2], E. Radenac[2], O. Rouzaud[2], P. Trontin[1], P. Villedieu[2]

[1]Claude Bernard Lyon 1 University.
Fluid Mechanics and Acoustics Laboratory (LMFA).
Lyon, France.

[2]ONERA
Multi-Physics Department for Energy (DMPE)
Toulouse, France

SLD, ice crystals, snowflakes : some definitions

SLD : Supercooled Large Droplet

- Droplet for which **D > 50 µm**.
- Complex interaction with the wall.

Definition	MVD range (μm)	Dmax range (μm)	No. of 30-s data points	MVD (μm)	Dmax (μm)
Freezing drizzle environments	<40	100–500	1469	20	389
Freezing drizzle environments	>40	100–500	335	110	474
Freezing rain environments	<40	>500	193	19	1553
Freezing rain environments	>40	>500	447	526	2229

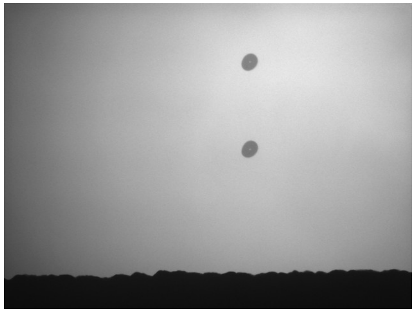

SLD, ice crystals, snowflakes : some definitions

Ice crystals :

- Ice particles **D ~ 100 µm**.
- Non sphericle particles.
- Present at high altitude and low temperature.
- Characterization of the existing liquid water.

SLD, ice crystals, snowflakes : some definitions

Snowflakes, aggregates :

- Predominance of aggregates (D_{max}>1mm)
- Low bulk density (~10 $kg.m^{-3}$)

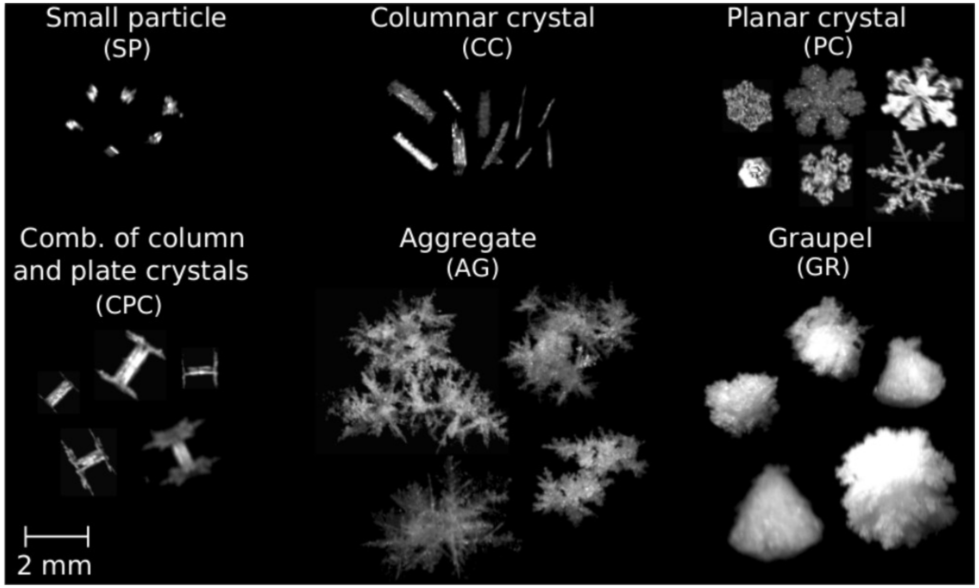

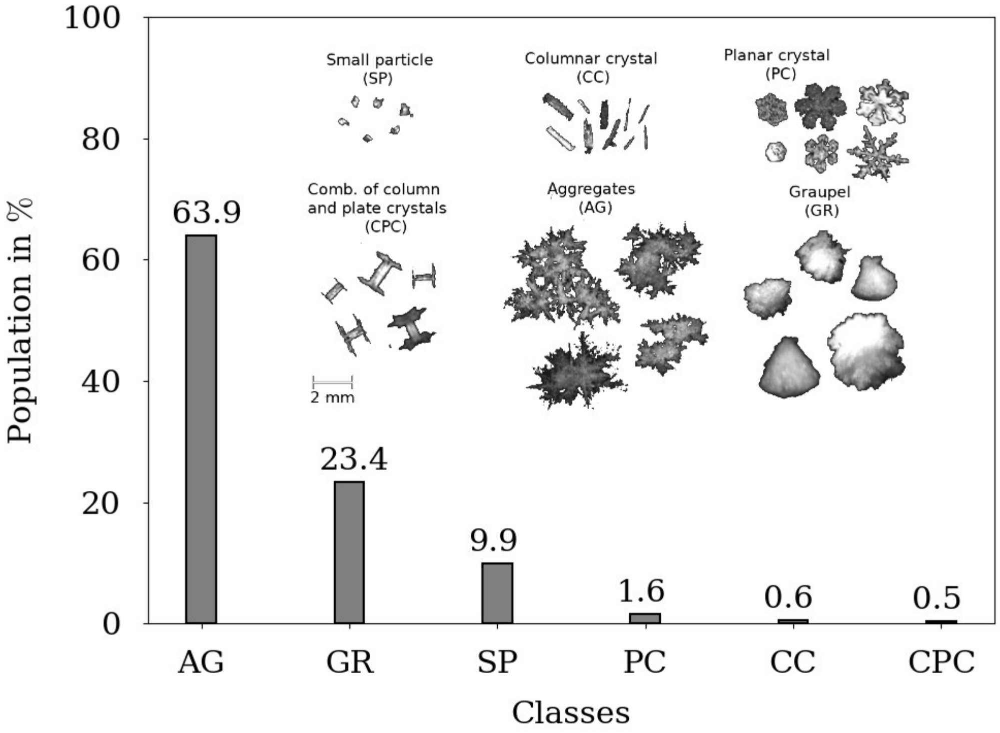

Classical icing limitations

Roselawn, USA, 1994

ATR 72-212

"The loss of control, attributed to a sudden and unexpected aileron hinge moment reversal, that occurred after a **ridge of ice accreted beyond the deice boots** while the airplane was in a holding pattern during which it intermittently encountered supercooled cloud and drizzle/rain drops, **the size and water content of which exceeded those described in the icing certification envelope.** The airplane was susceptible to this loss of control and the crew was unable to recover."

- Unusual droplet diameter and liquid water content.
- Ice protection systems (IPS) poorly qualified for the regime of large droplets.
- **Supercooled large droplets (SLD).**

Classical icing limitations

AF 447 flight Rio de Janeiro – Paris (2009).

Conclusions from the BEA report :

- « There was an inconsistency between the measured velocities, probably due to the **clogging of the Pitot probes by ice crystals** »

- « The exact composition of cloud masses in the atmosphere above 30,000 feet is poorly known, especially with respect to the **level of supercooled water/ice crystals sharing** and in particular their size »

- A particular behavior of ice crystal with respect to liquid droplets in the accretion process.
- The combined presence of liquid water and solid ice leads to an additional complexity in the consideration of the ice crystal regime.
- **Ice Crystal Icing (ICI)** regime.

Classical icing limitations

HH-65A Dolphin

Problems encountered during the test phase (admiral James S. Gracey, US, 1986 : « The snow problem was that the **snow accumulates in an inlet and then breaks off** »

Icing in **snowy conditions**.

Specificities for SLD, ice crystals and snow in the accretion process

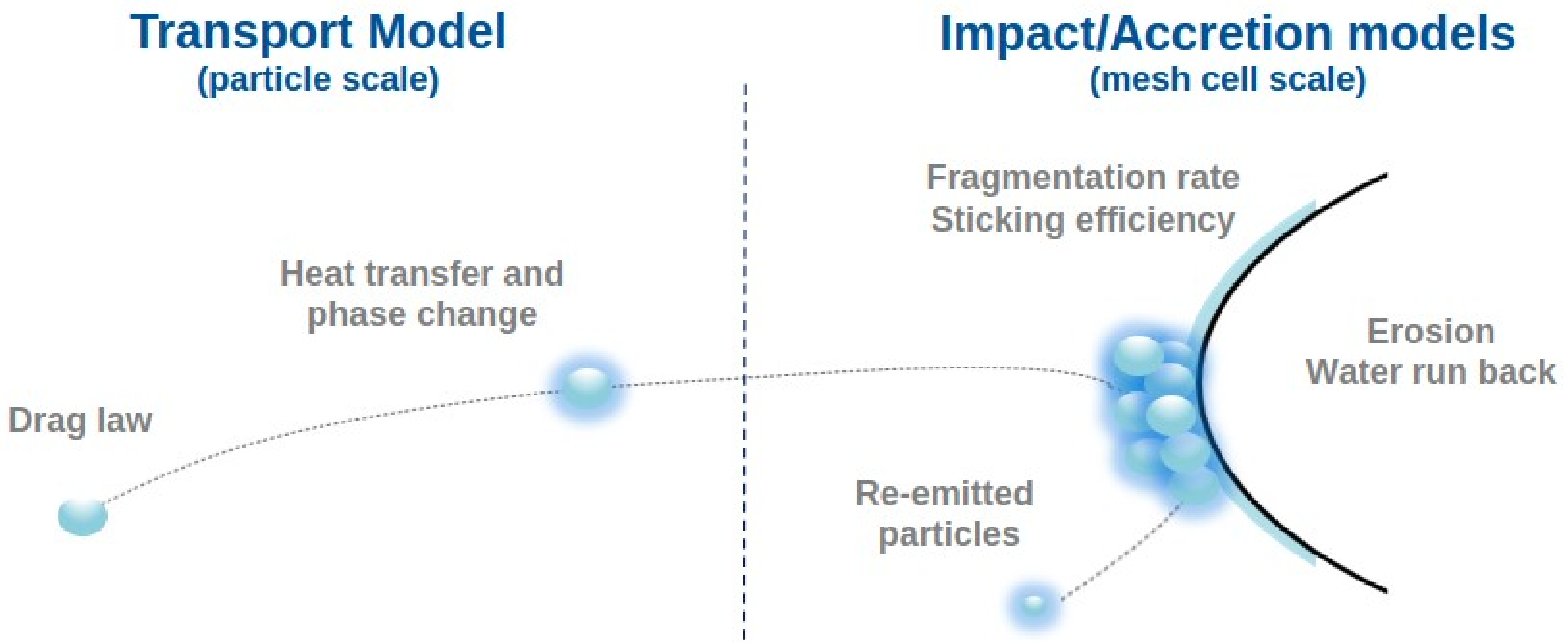

PhD thesis, B. Aguilar.

Specificities for SLD, ice crystals and snow in the accretion process

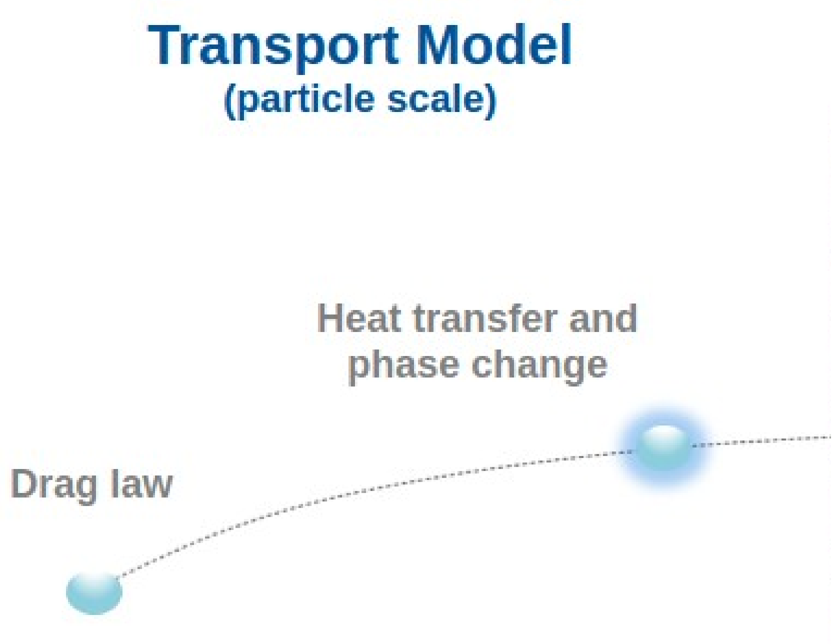

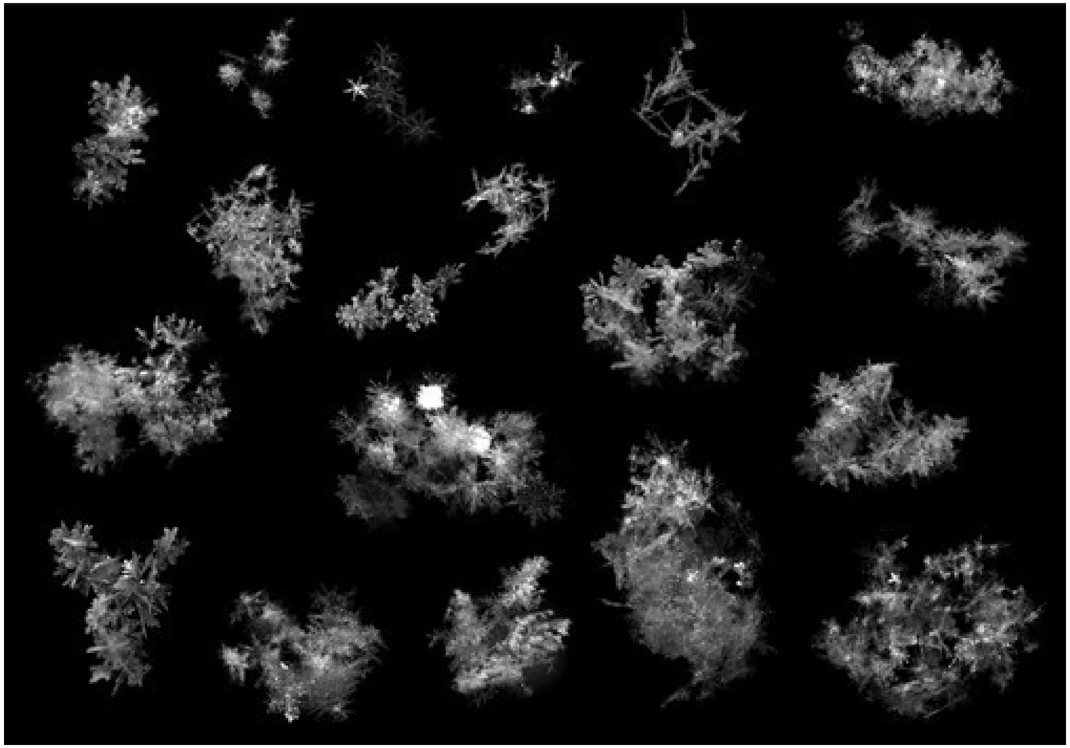

- Wide variety of shapes for **snowflakes and aggregates.**
- Very different from a droplet and even from an ice crystal.
- **Non-spherical** particle with low bulk density ⇒ Adapt models for drag coefficients and heat and transfers.

Specificities for SLD, ice crystals and snow in the accretion process

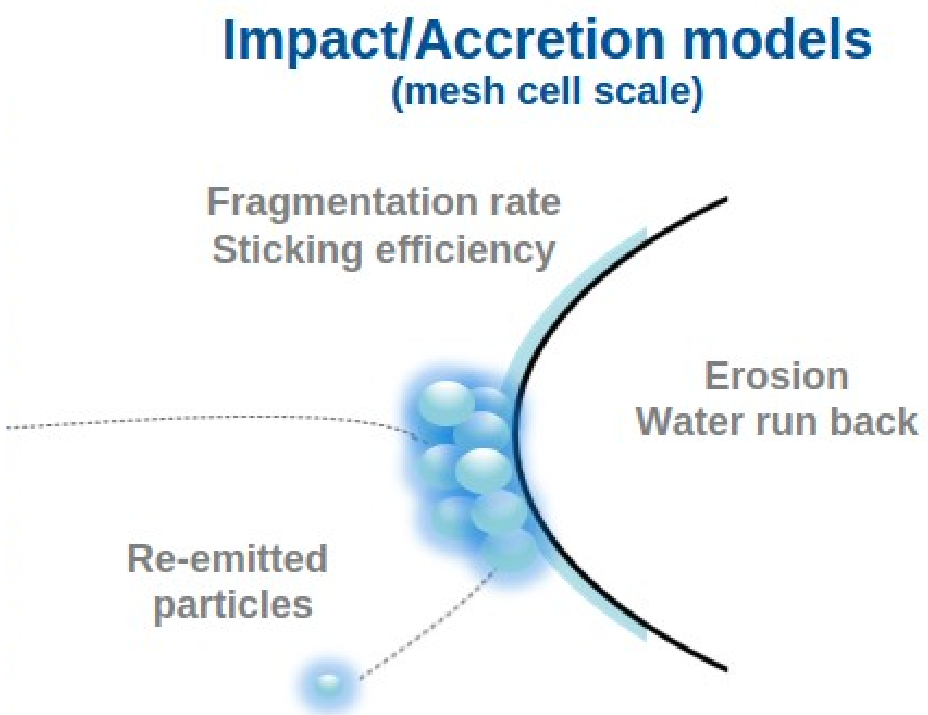

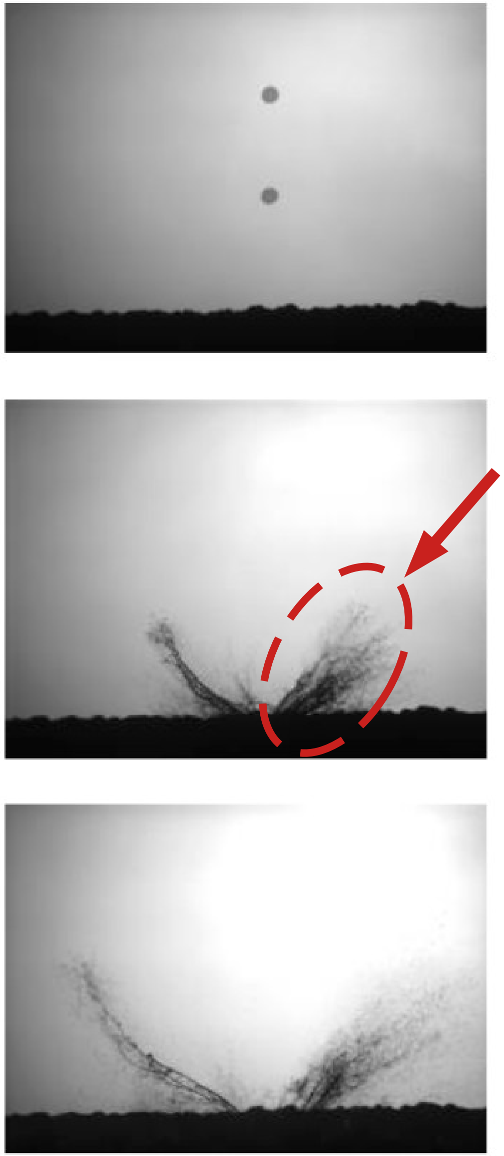

- Partial deposit on the wall
- Re-emitted particles

Impact of a **SLD** (D=330µm, V=150m/s, $We \approx 10^5$) on an iced surface. (PhD thesis, T. Alary).

Specificities for SLD, ice crystals and snow in the accretion process

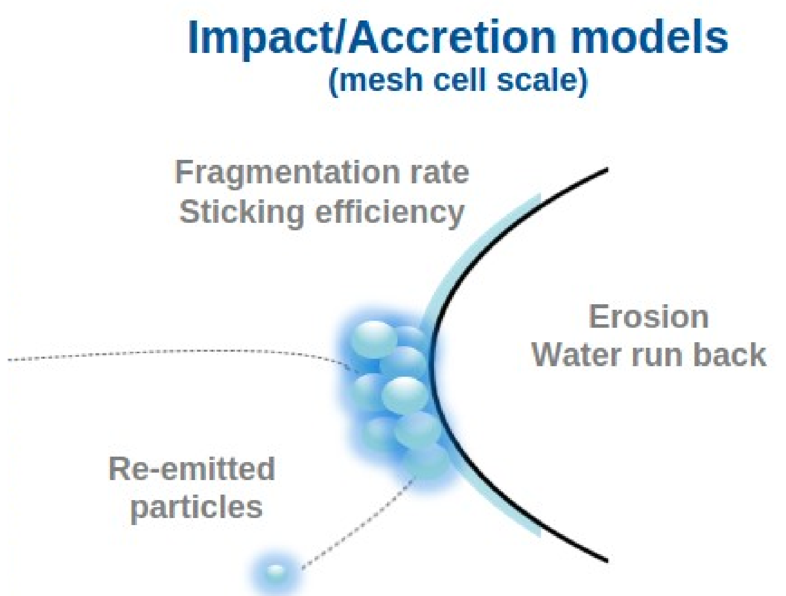

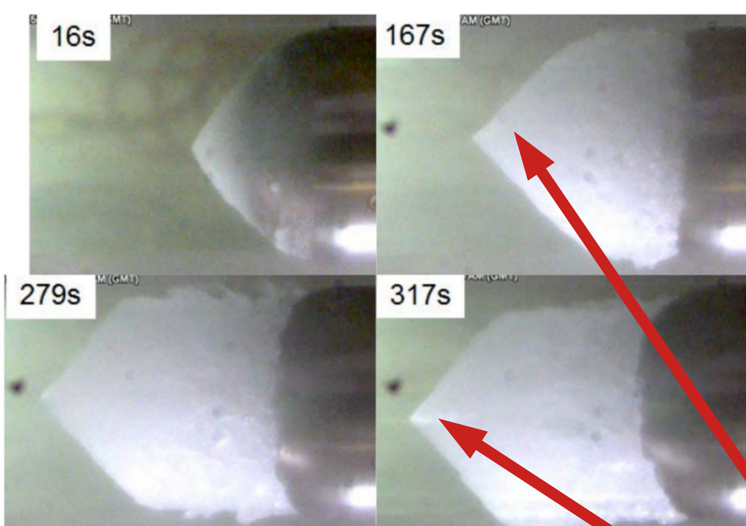

Run 699 : M = 0.48, MVD = 28 µm

Currie, AIAA, 2016

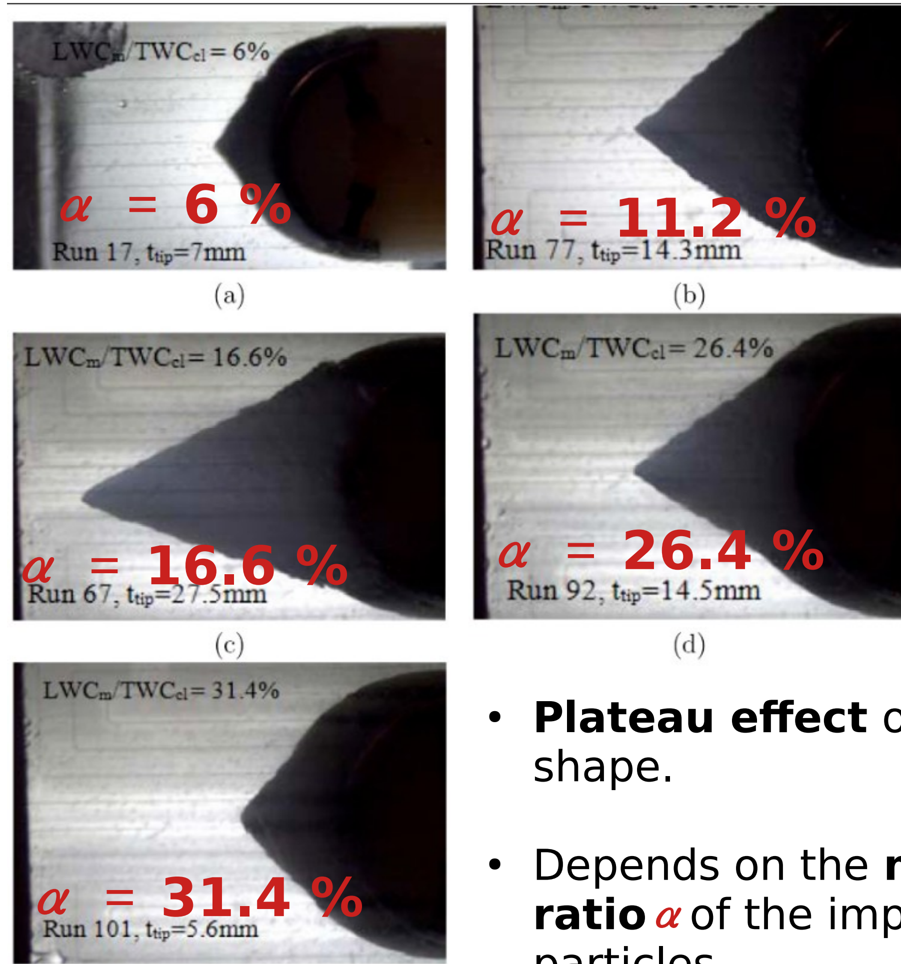

- **Plateau effect** on the ice shape.
- Depends on the **melting ratio** α of the impacting particles.

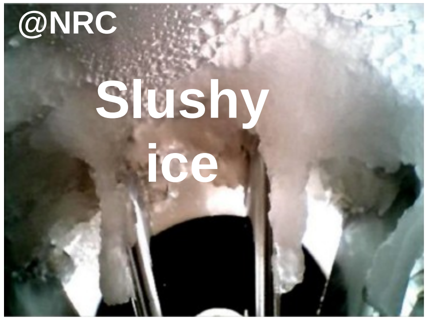

- Conical ice shapes.
- Typical of **ice crystal** icing (ICI) with erosion.

Illustrative example : ice crystal icing in an engine

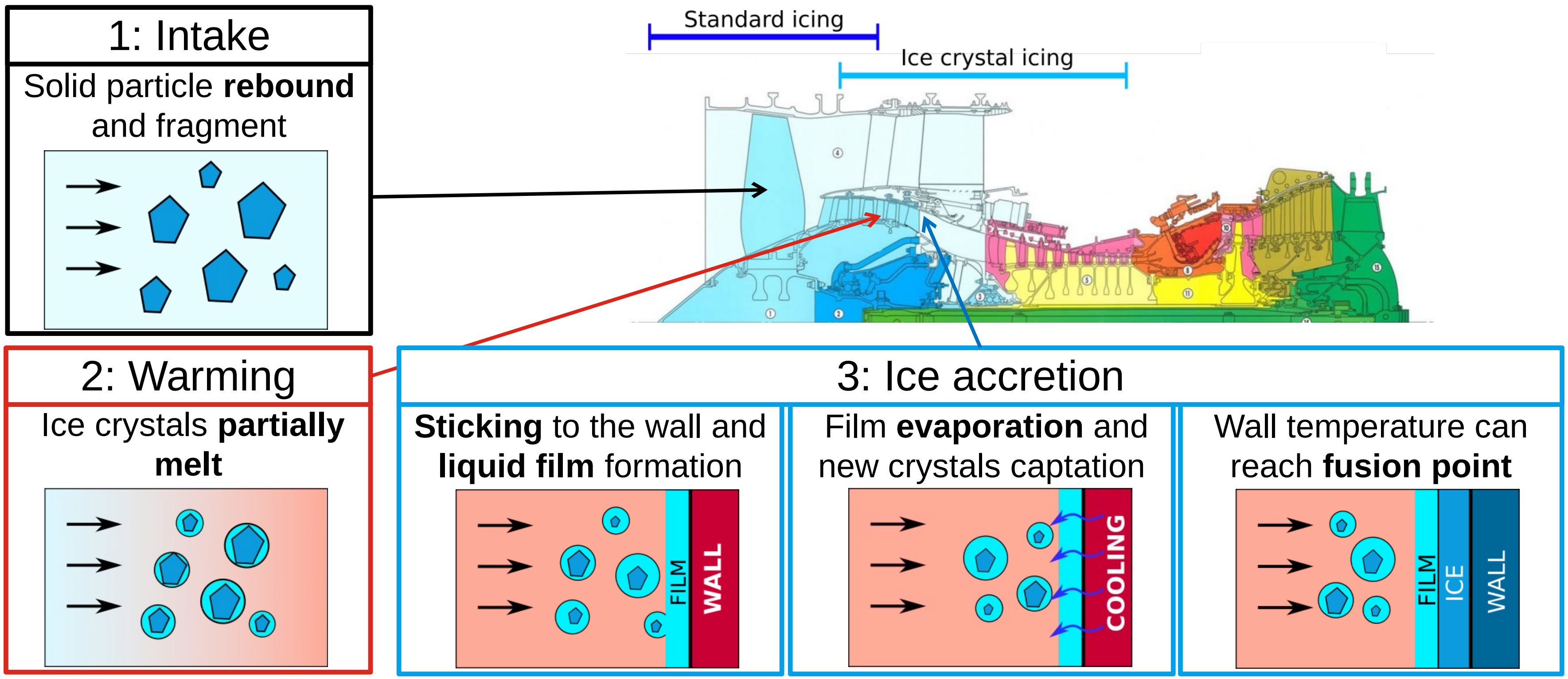

Charton, SAE, 2019.

Illustrative example : ice crystal icing in an engine

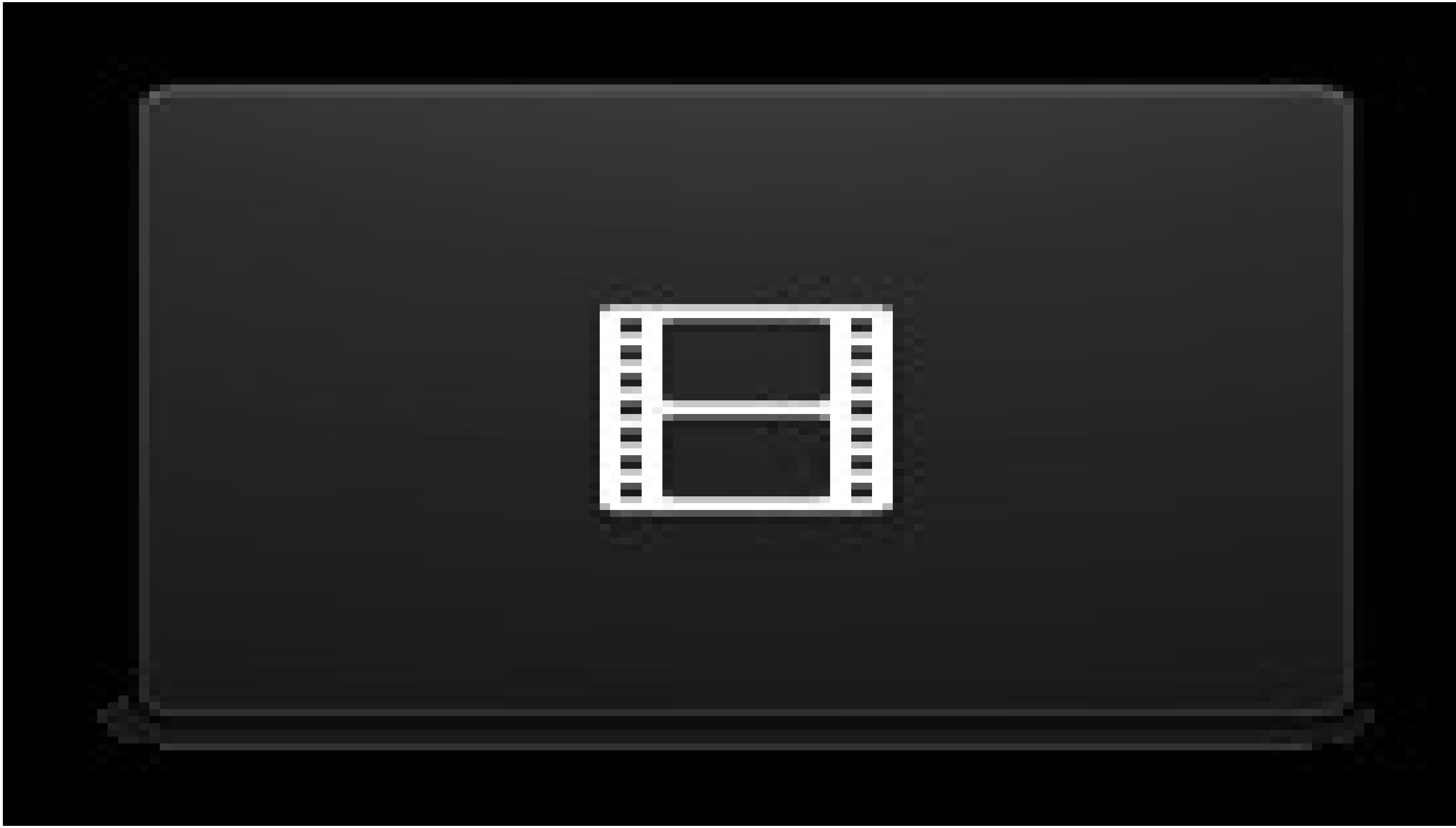

Outline

1) Trajectory model adaptation for SLD, ice crystals and snowflakes.

2) Impact model adaptation for SLD, ice crystals and snowflakes.

3) Accretion model adaptation for SLD, ice crystals and snowflakes.

Outline

1) Trajectory model adaptation for SLD, ice crystals and snowflakes.

2) Impact model adaptation for SLD, ice crystals and snowflakes.

3) Accretion model adaptation for SLD, ice crystals and snowflakes.

Particle geometric description

- Given the altitude (temperature) and the supersaturation level, **different shapes** for the ice crystals are observed

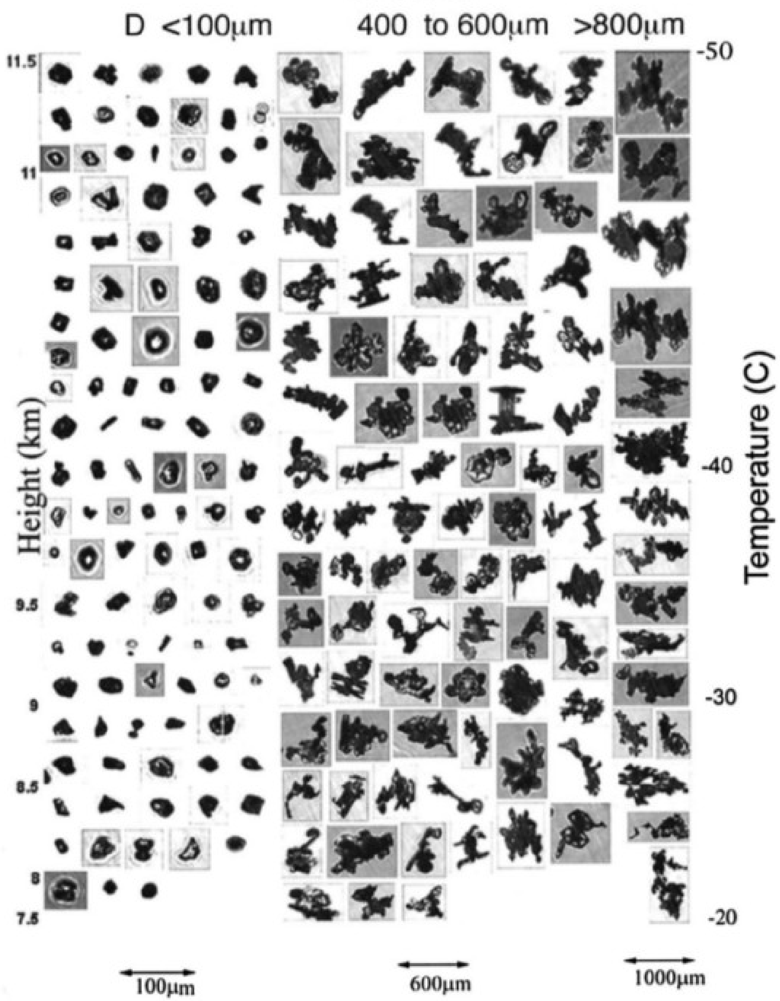

Examples of particles vs. altitude (km) and temperature (∘ C) imaged in three size ranges(< 100, 400 − 600, > 800 µm by CPI probe on August 22, 1999. Heymsfield *et al.*

- Several global geometric descriptors are used:
  - ✓ Particle **equivalent diameter** d_p
  - ✓ Particle **sphericity** Φ
  - ✓ Particle **crosswise sphericity** $\Phi^{\perp}$

Particle geometric description

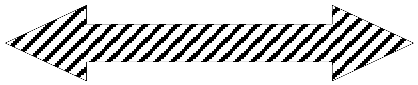

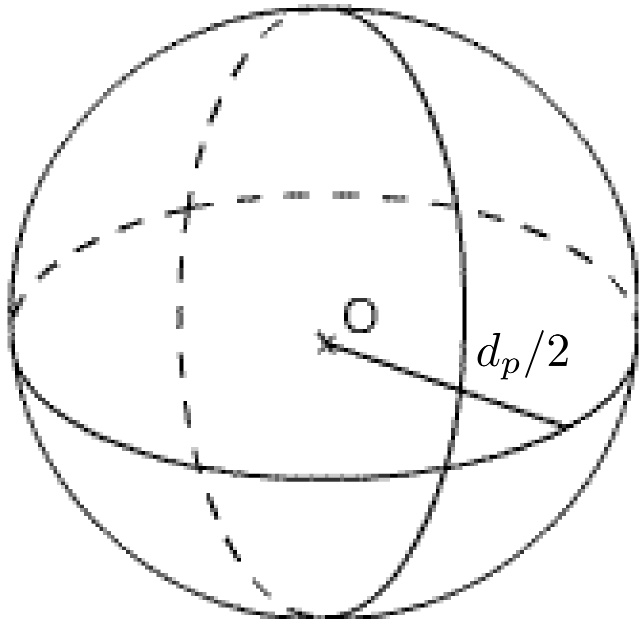

Snowflake :

- Volume V_p
- External surface A_p

$$d_p = \left(\frac{6V_p}{\pi}\right)^{1/3}$$

$$\Phi = \frac{\pi d_p^2}{A_p} < 1$$

Particle geometric description

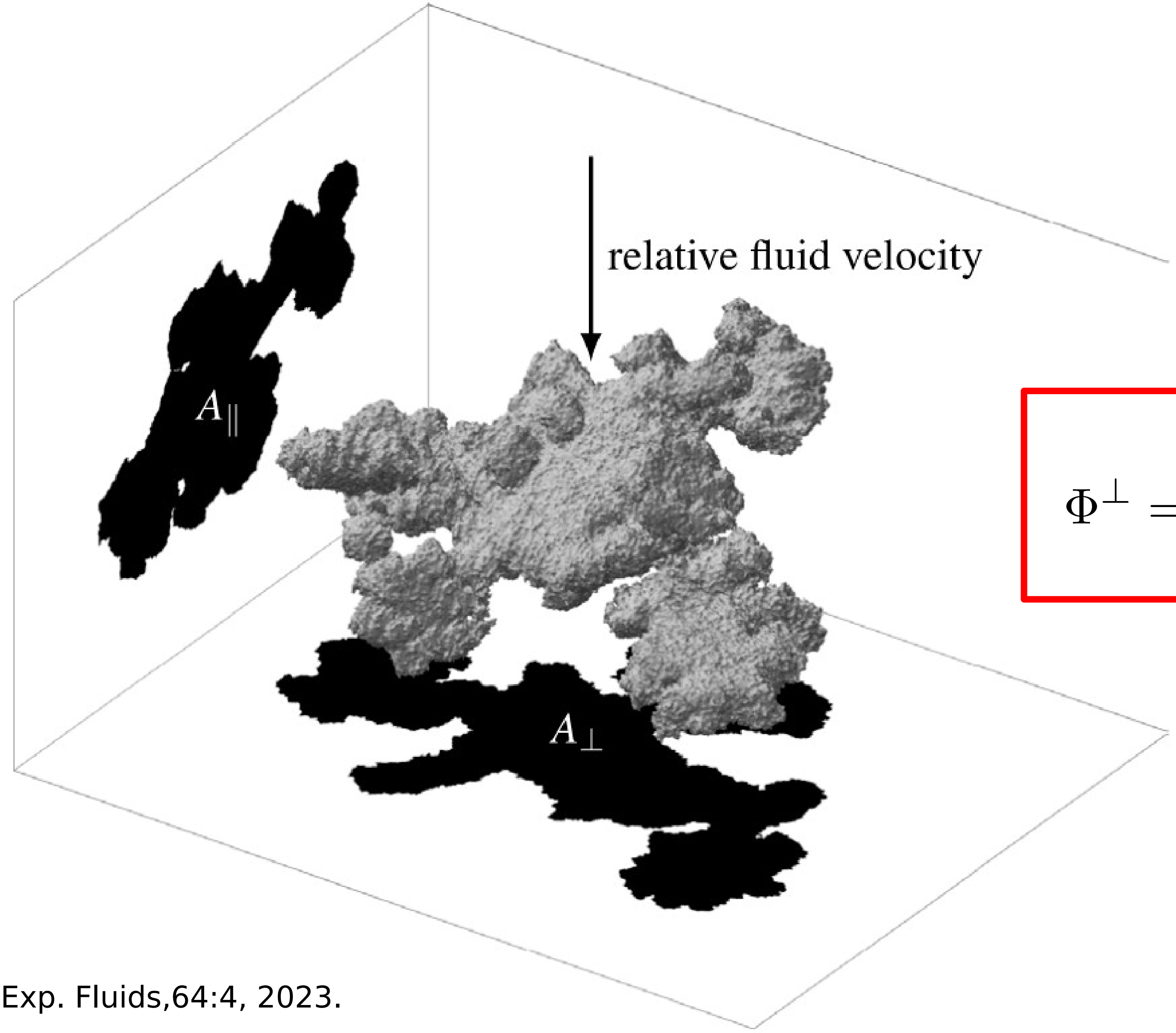

$$\boxed{\Phi^{\perp} = \frac{\pi d_p^2/4}{A_p^{\perp}}}$$

Köbschall *et al.*, Exp. Fluids,64:4, 2023.

Trajectory models for non sphericle particles

Drag models : $C_d = C_d\left(Re_p, \Phi, \Phi^{\perp}\right)$

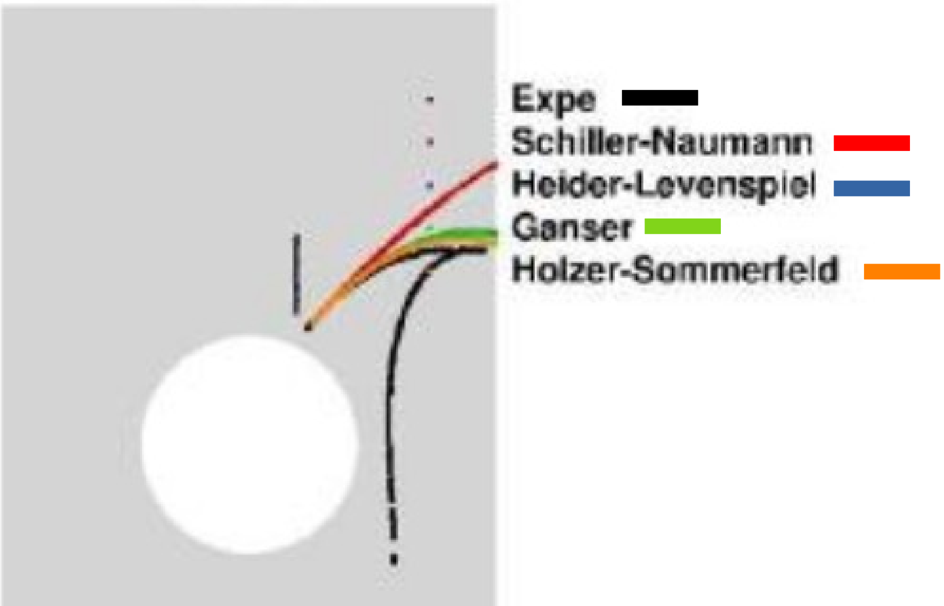

- **Ice crystals**
- Large sphericities ($\Phi > 0.7$)

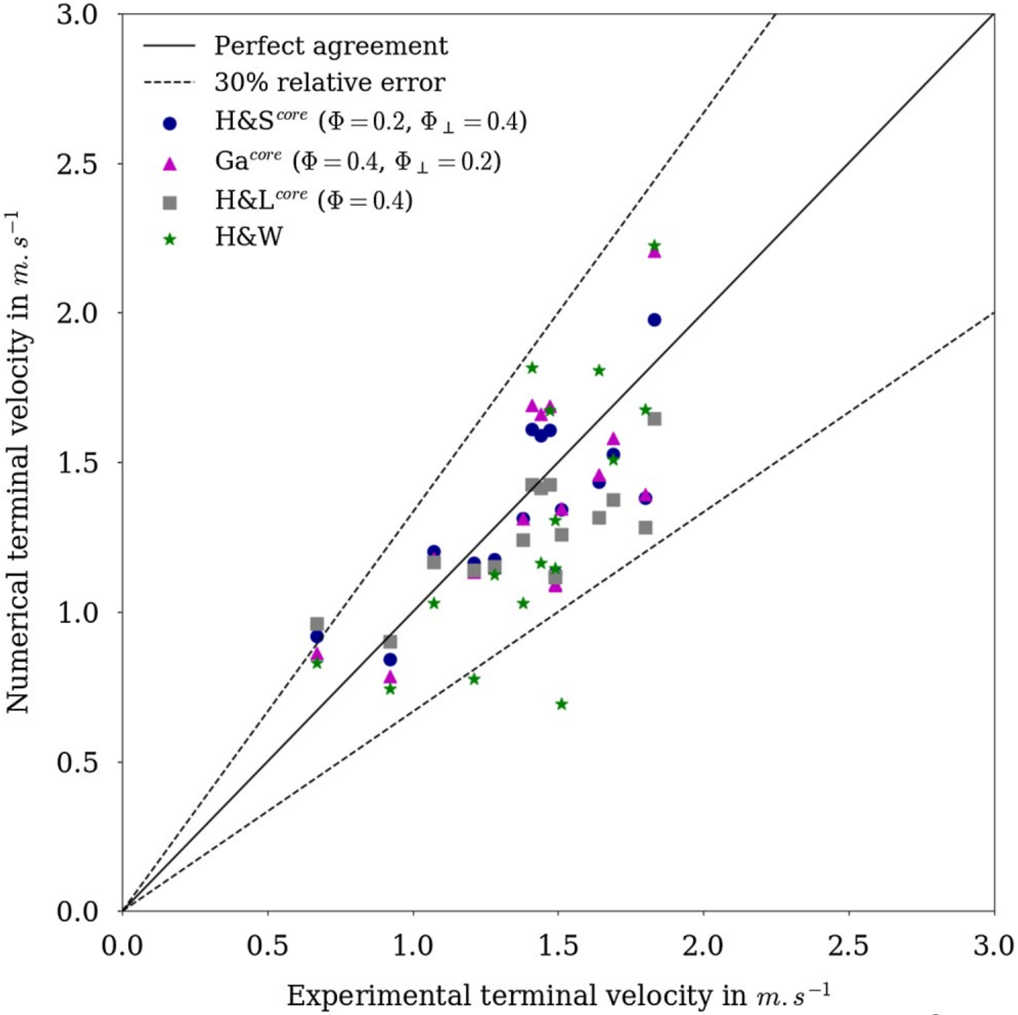

- **Light aggregates** ($\rho_p \sim 10\,\mathrm{kg.m^{-3}}$)
- Need low values for Φ to apply drag models validated for ice crystals..

Aguilar *et al.*, AIAA J. 2022.

Trajectory models for non sphericle particles

An adaptation for **light snow aggregates**

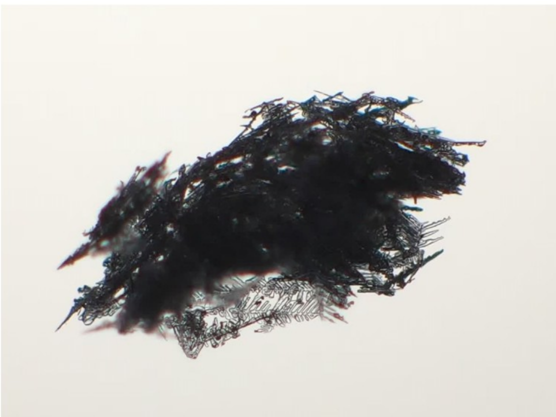

a) Grayscale image of a snowflake

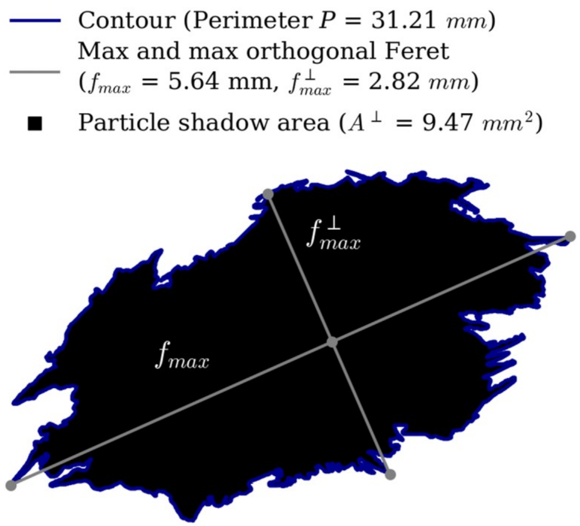

(b) Postprocessed image

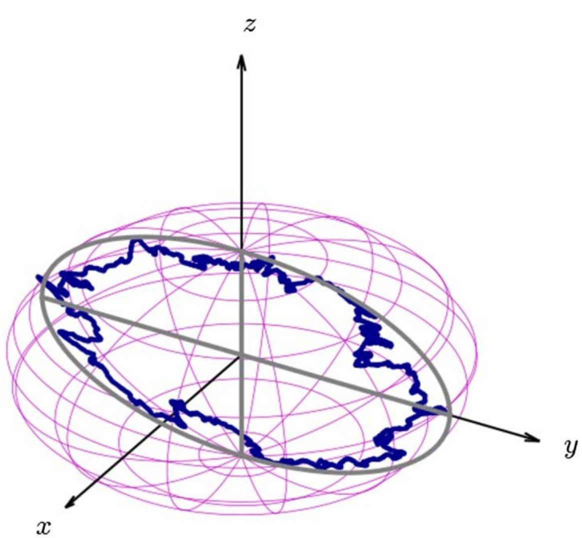

a) Oblate spheroid reconstruction

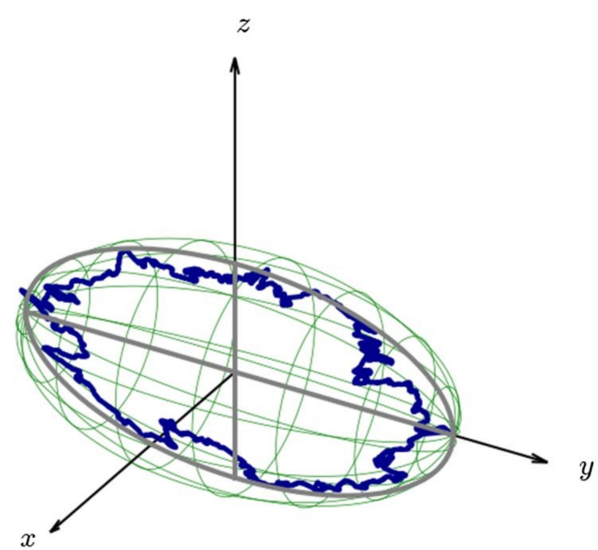

b) Prolate spheroid reconstruction

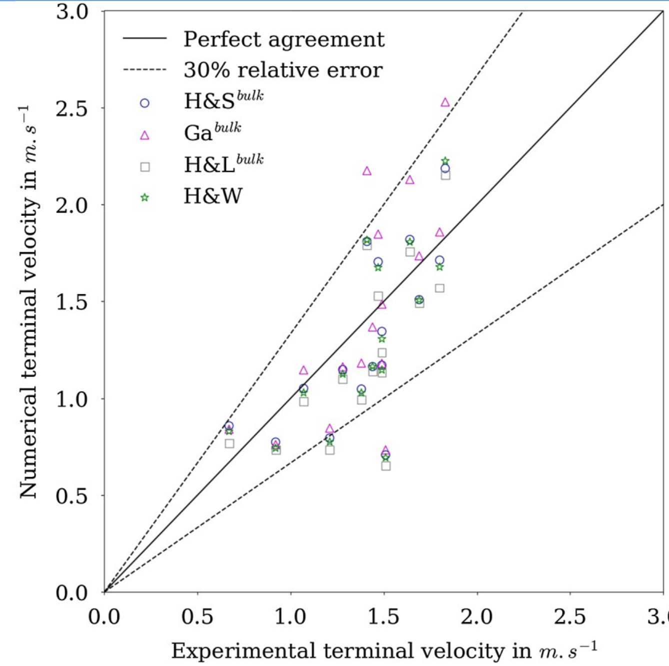

a) Oblate spheroid reconstruction

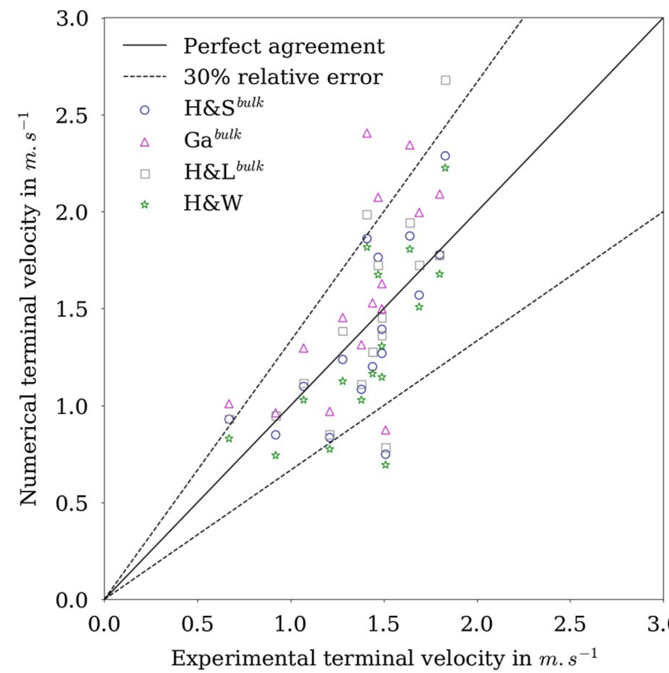

b) Prolate spheroid reconstruction

Aguilar *et al.*, IJHMT. 2023.

Heat and mass transfer models for non sphericle particles

$$L_f \frac{d}{dt}\left(Y_l \cdot m_p\right) = \pi d_p \frac{Nu}{\Phi} k_a \left(T_a - T_0\right) - \dot{m}_{\mathrm{ev}} L_s$$

$$\frac{d}{dt}\left(m_p\right) = -\dot{m}_{\mathrm{ev}}$$

$$Nu = 2\sqrt{\Phi} + 0.55\sqrt{Re_p}\,Pr^{1/3}\Phi^{1/4}$$

Modified Frössling correlation for non-spherical particles

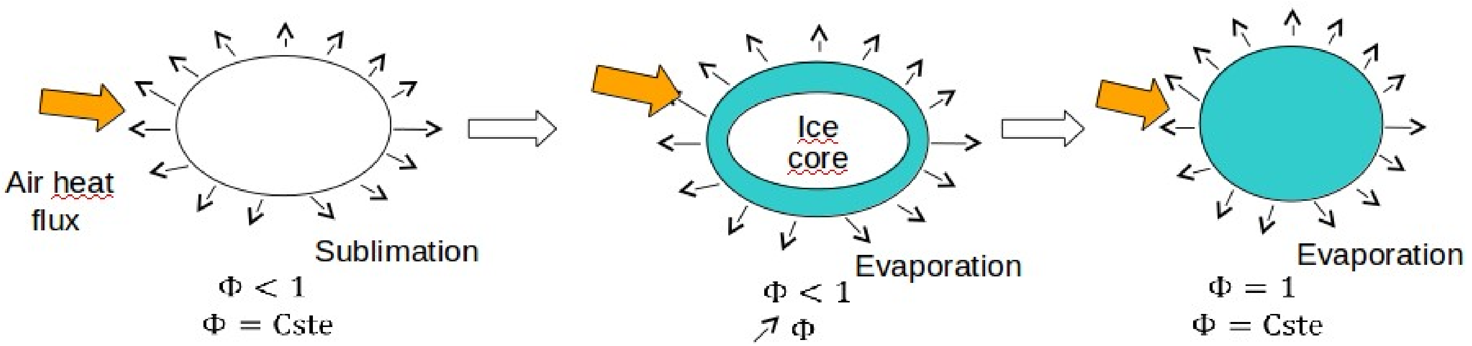

Increased melting times due to evaporative cooling at low relative humidity. Poorly estimated by the model.

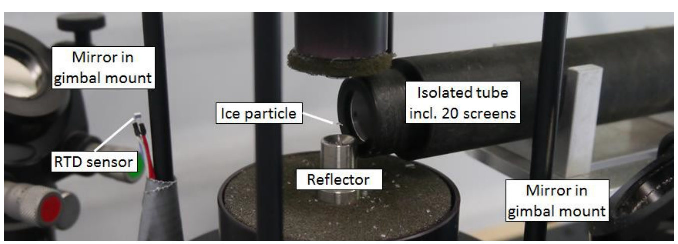

Accoustic levitator (HAIC, AGI)

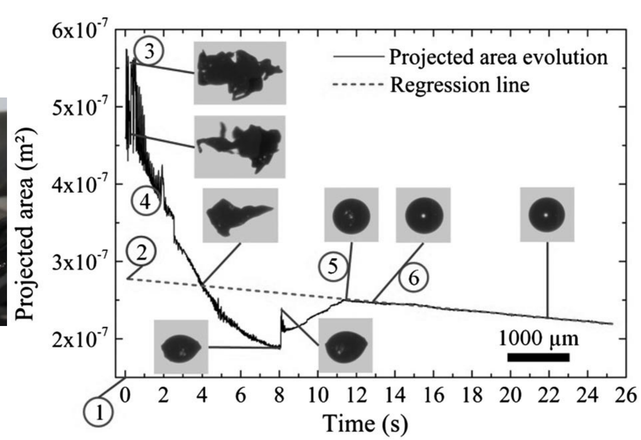

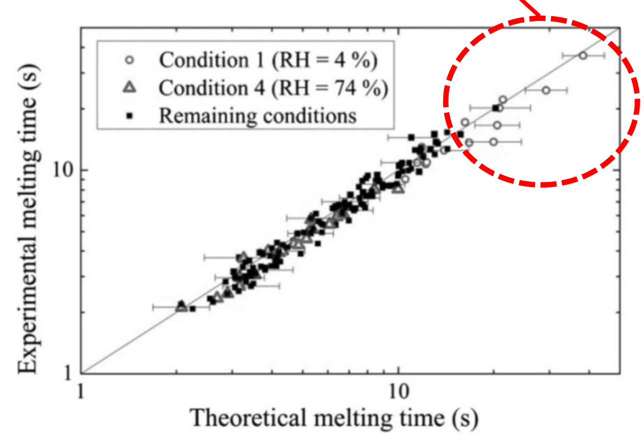

Non-spherical **ice crystal** particles.

Hauk et al. *J. of Thermophysics and Heat Transfer*, 2016

Heat and mass transfer models for non sphericle particles

Adaptation for the case of **light snowflakes** :

- Strong evolution of the particle density between the dry bulk density $\rho_p^{\mathrm{bulk}} \sim 10\,\mathrm{kg.m}^{-3}$ and the liquid water ($\rho_l = 997\,\mathrm{kg.m}^{-3}$).

- **Non linear** evolution.

- A need to adapt the models derived from ice crystals.

Aguilar et al. *IJHMT*, 2023

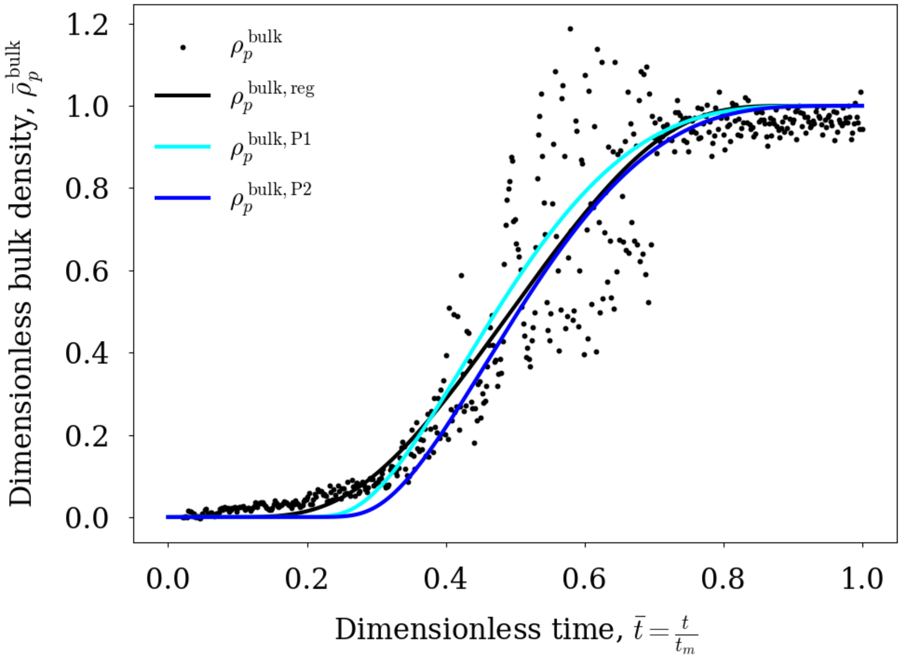

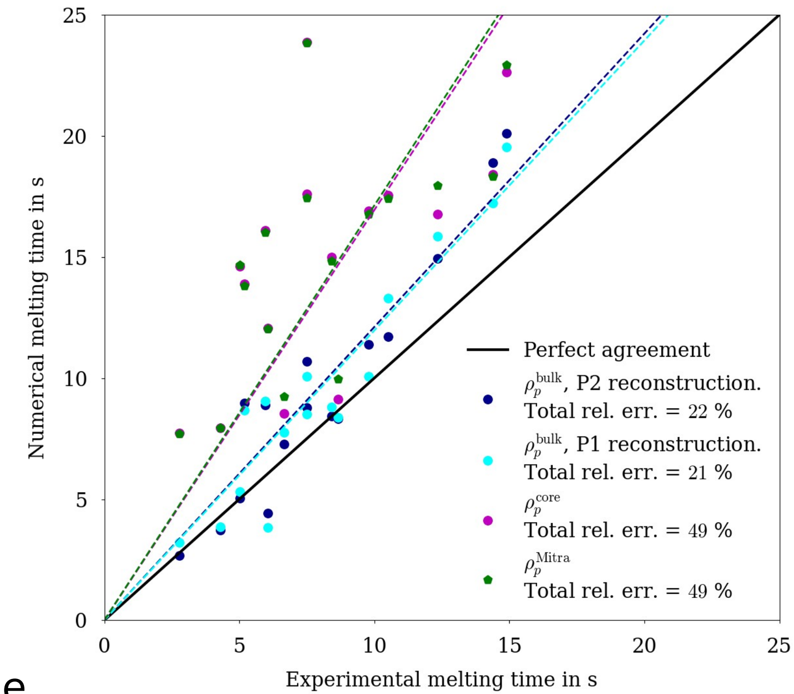

Y_l : particle liquid fraction

$$\rho_p^{\mathrm{ICI}} = \left(\frac{Y_l}{\rho_l} + \frac{1 - Y_l}{\rho_{p0}^{\mathrm{ICI}}}\right)^{-1}$$

$$\bar{\rho}_p^{\mathrm{snow}} = \frac{1}{2} + \frac{1}{2}\tanh\left(\frac{c_1}{1 - Y_l^{c_2}} - \frac{c_1}{Y_l^{c_2}}\right)$$

Outline

1) Trajectory model adaptation for SLD, ice crystals and snowflakes.

2) Impact model adaptation for SLD, ice crystals and snowflakes.
   a) SLD
   b) Ice crystals

3) Accretion model adaptation for SLD, ice crystals and snowflakes.

Key points

A simple underlying problem:

- Estimate the **sticking efficiency** ε_s
- Characterization of the **secondary (re-emitted) particles**

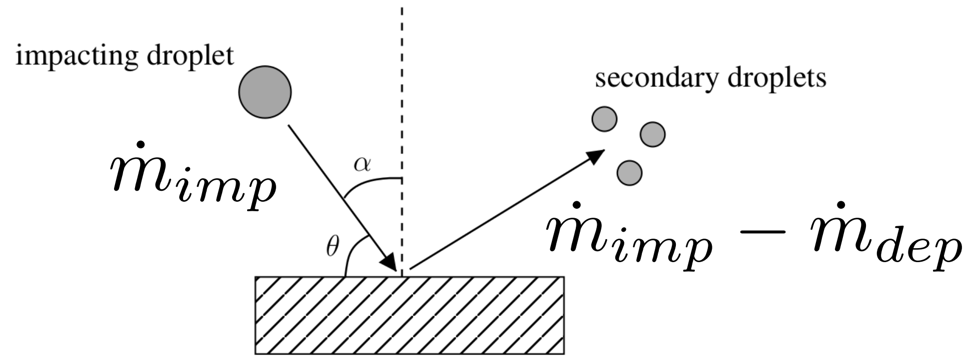

$$\varepsilon_s = \frac{\dot{m}_{dep}}{\dot{m}_{imp}}$$

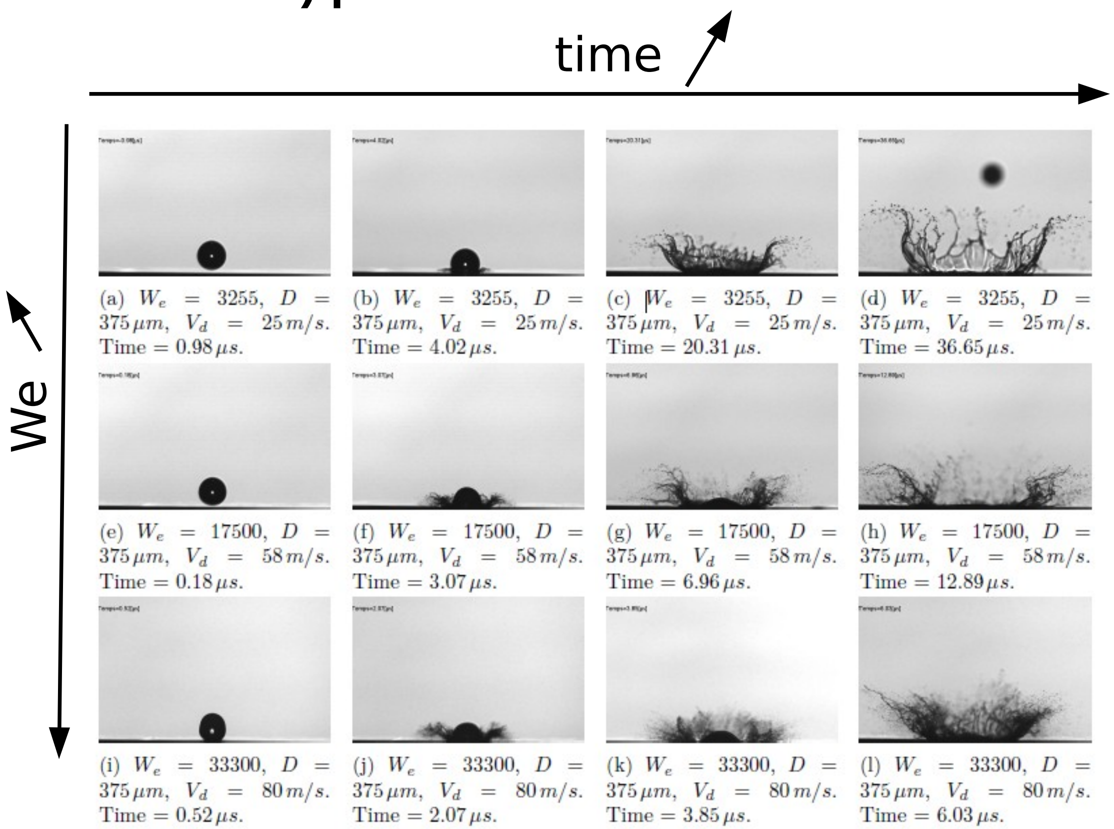

SLD impact (standard conditions) on a clean alumium wall.

Pictures from P. Berthoumieu and V. Bodoc (PHYSICE2)

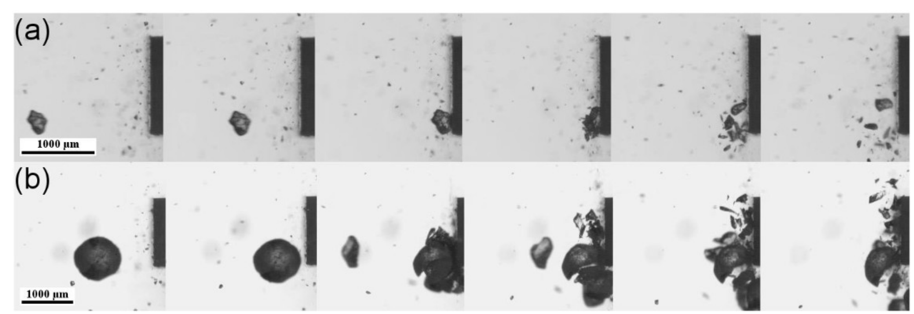

Impact of a **fully glaciated ice particle** on a wall.
Impact velocity between 40 and 50 m/s.

PhD thesis of T, Hauk (HAIC).

Impact for SLD : regime of interest for aeronautical applications

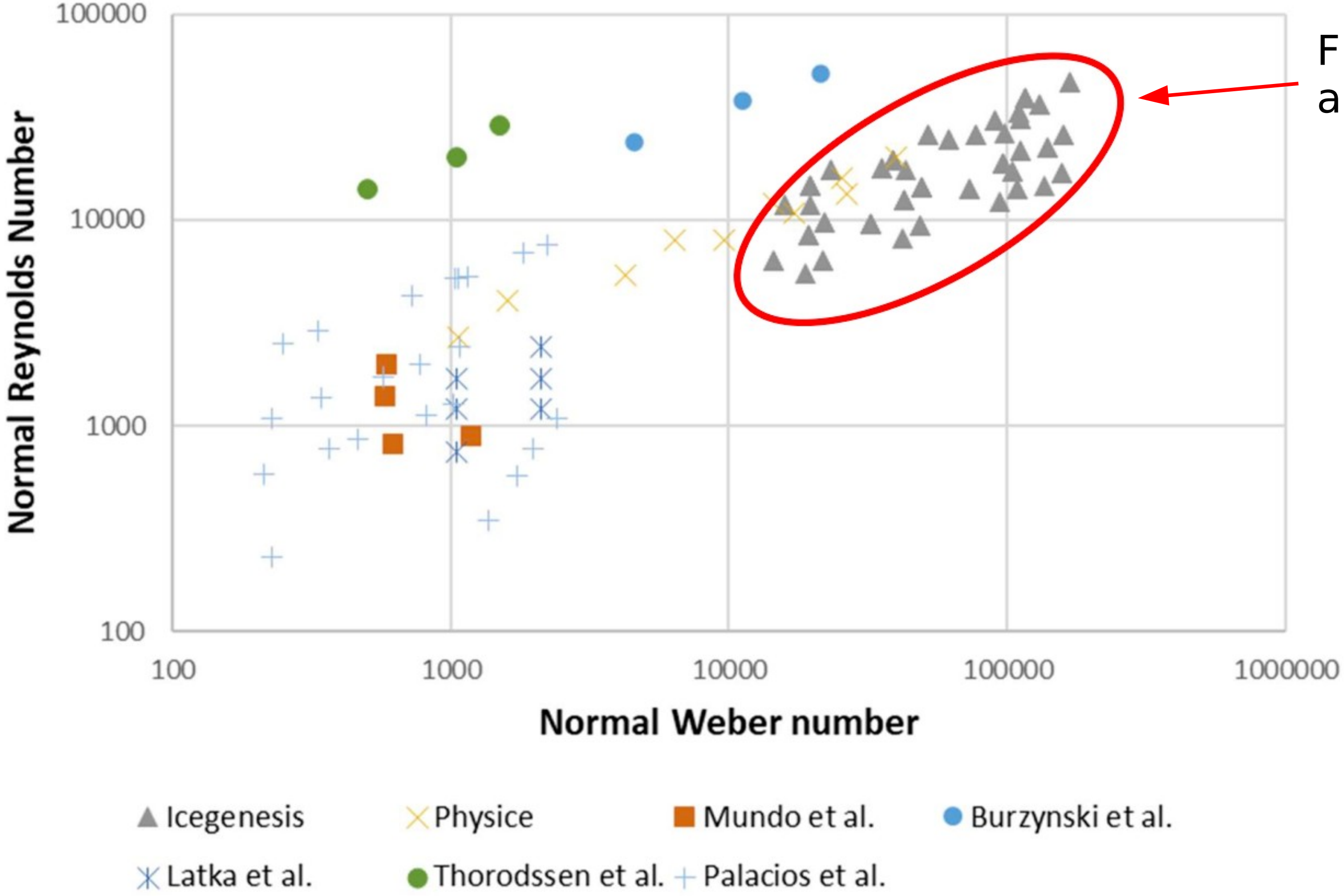

Flight regime of interest for aeronautical applications.

Sticking efficiency for SLD

$$U_\infty = 100m/s \quad T_\infty = 0^oC \quad \text{chord} = 145mm$$

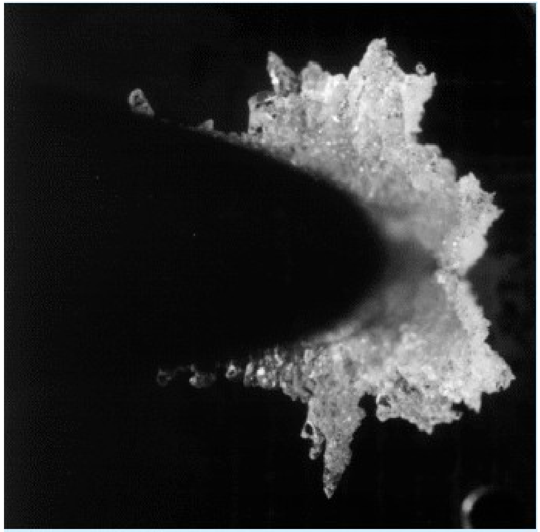

D=60µm

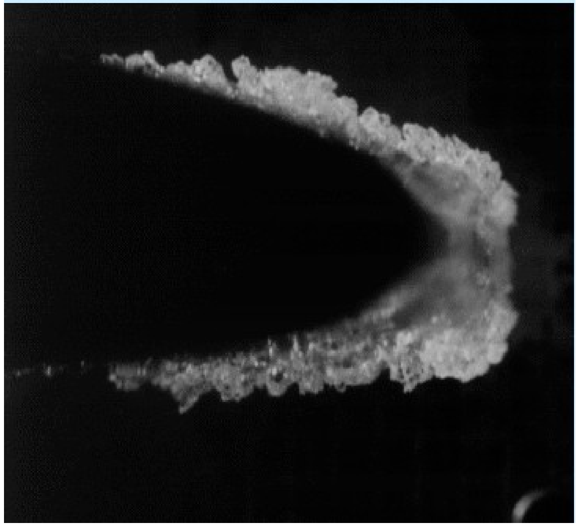

D=100µm

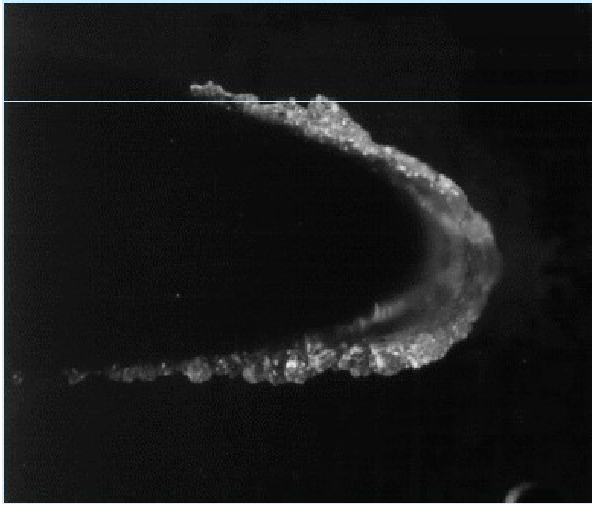

D=200µm

- Estimation of ε_s is paramount for **ice shape prediction.**
- Impact **beyond** the ice protection system due to the greater inertia of the droplets.
- The experimental estimation of ε_s is not straightforward.

Sticking efficiency for SLD: indirect measurement

$$\varepsilon_s = \frac{\dot{m}_{dep}}{\dot{m}_{imp}}$$

Experimentally estimated

Numerically (from simulations) estimated

- $\dot{m}_{imp} = \beta \dot{m}_{\infty}$ accurately estimated by a trajectory solver.

- More sensitive estimation for $\dot{m}_{dep}$:
  - Collection of the water not re-emitted as droplets by a **collecting tank**.
  - Use of an **absorbent blotter paper** to retain the collected water.
  - For rime ice conditions (low temperature ~ -10°C), estimate **ice accretion thickness.**

Sticking efficiency for SLD: indirect measurement (collecting tank)

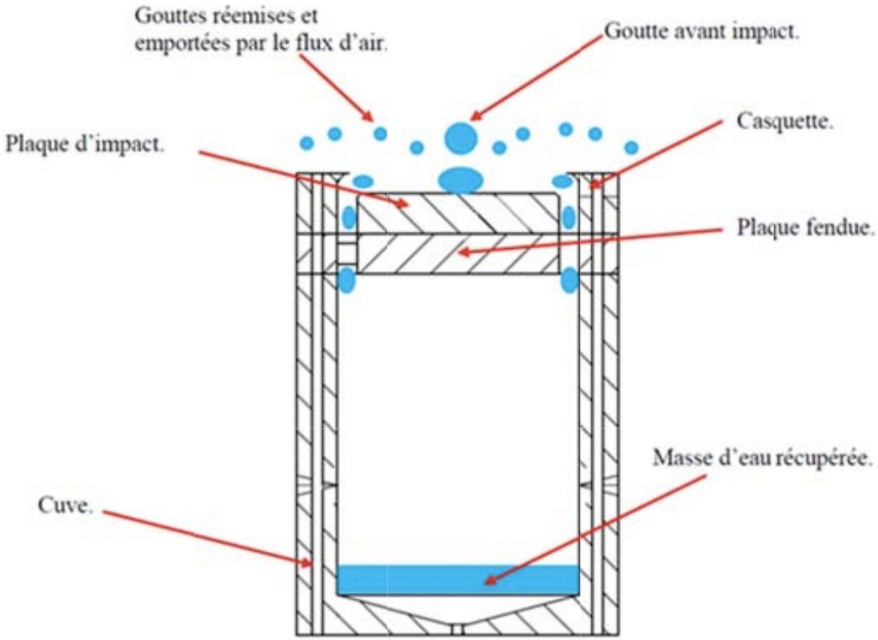

Main drawbacks :

- Strong influence of the **air flow** (surface sweeping)
- Control the **humidity level** and the amount of water evaporated.
- Difficult to **discriminate** between deposits from the primary impact and deposits from the local secondary re-impact.
- All the more precise as the impact occurs at low velocity.

Sticking efficiency for SLD: indirect measurement (absorbent blotter paper)

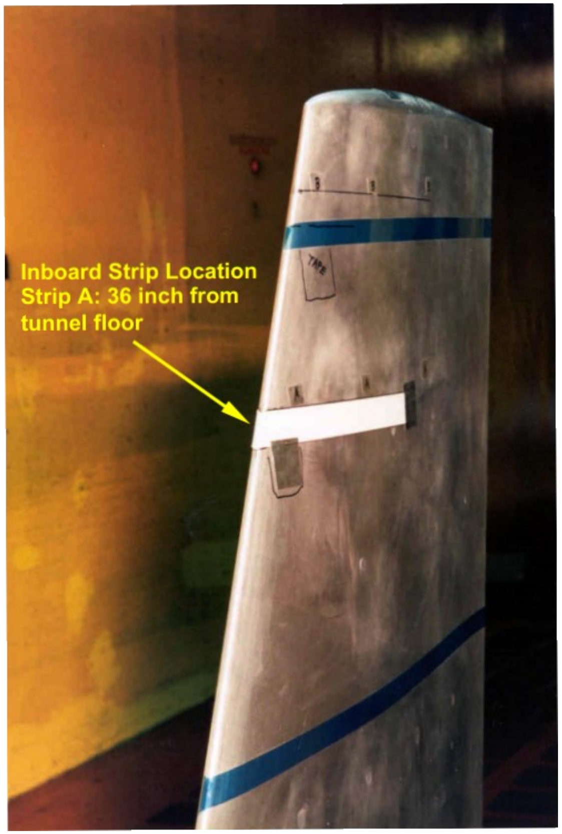

Papadakis et al., NASA/TR 2002-211700 (2002)

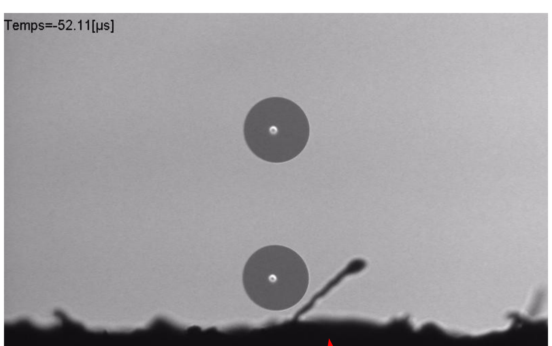

Blotter paper

Main drawbacks :

- Strong influence of the **absorbent properties** of the blotter paper.

- **Overestimation** of ε_s (in particular its asymtotic part) :
  - ~0.85 for blotter paper (normal impact).
  - ~0.6 for aluminium (normal impact)

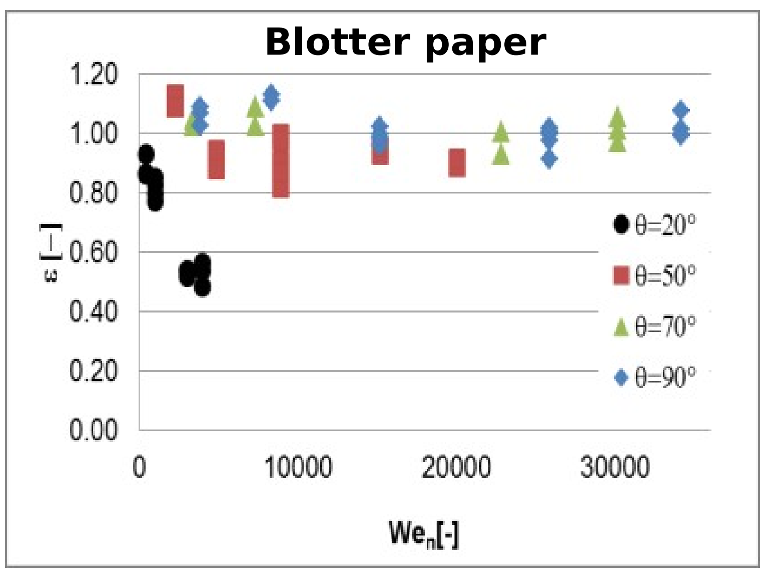

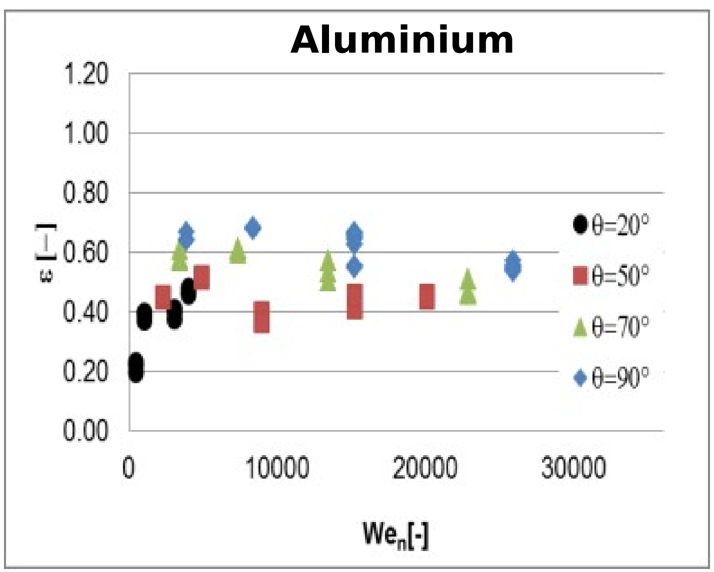

Sticking efficiency for SLD: indirect measurement (estimate ice accretion thickness)

$$\dot{m}_{acc} = \dot{m}_{dep} - \cancel{\dot{m}_{evs}} - \cancel{\dot{m}_{rb}}$$

disregarded =0 for rime ice conditions

$$\dot{m}_{dep} = \dot{m}_{acc} = \frac{\rho_{ice} h_{ice}}{t}$$

ρ_{ice} : rime ice density

h_{ice} : ice thickness

t : accretion time

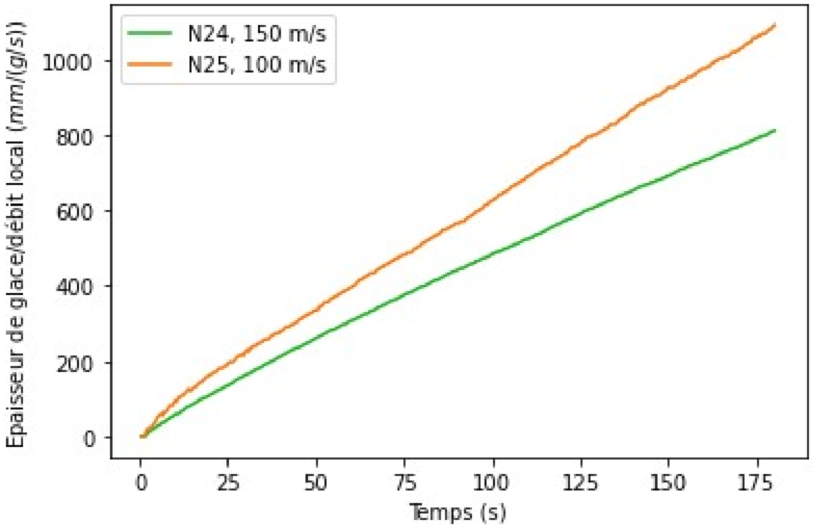

Main drawbacks :

- Need for geometries that minimize local re-impact.
- Need to know the **rime ice density**.

Model for SLD sticking efficiency

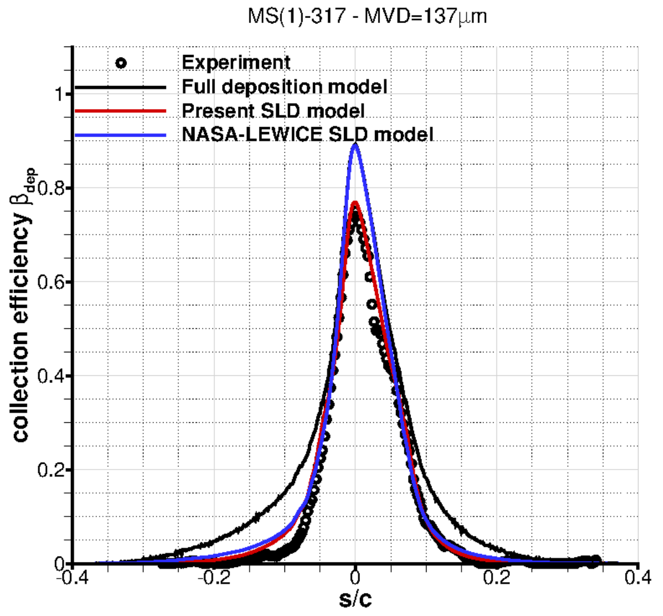

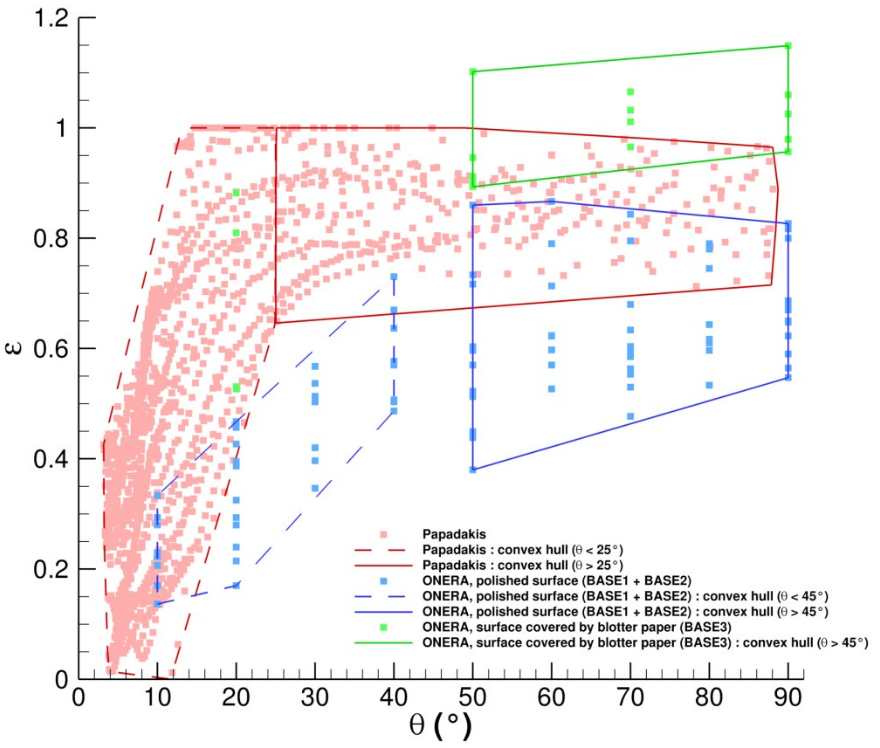

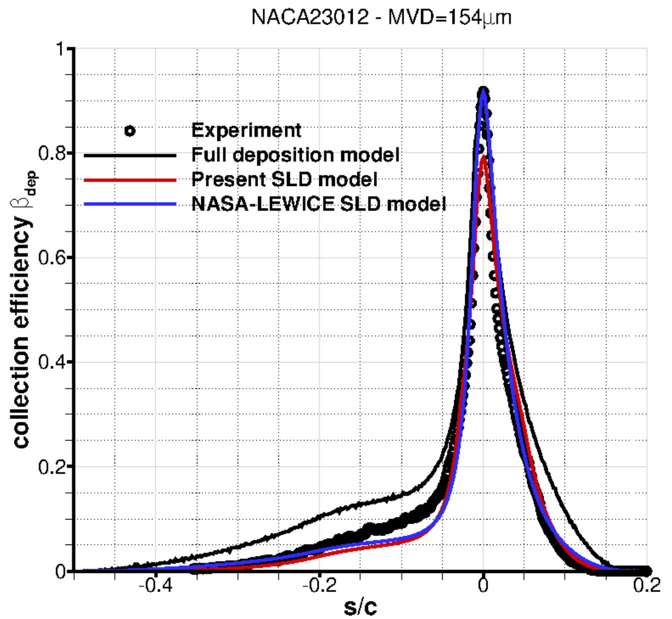

- One more model in the zoology of the models for ε_s near the leading edge.
- Improvement of the prediction of the **impingement limits**.
- Two zones:
  - Linear for grazing impacts (bouncing)
  - An asymptotic behavior. **High dependence on the nature of the impacted wall.**

Sticking efficiency for ice crystal

Fundamental point: role of **liquid water** in the collection of ice crystals. Source of the **liquid water**:

1) Impacting **partially melted** ice particles (**glaciated regime**) or **solid ice particles + supercooled droplets** (**mixed phase regime**)

2) **Capillary ascent** of the liquid water at the wall obtained from ice melting due to heat flux at the wall (heated wall)

3) Warm environment (air) with $T_{wb} > 0$

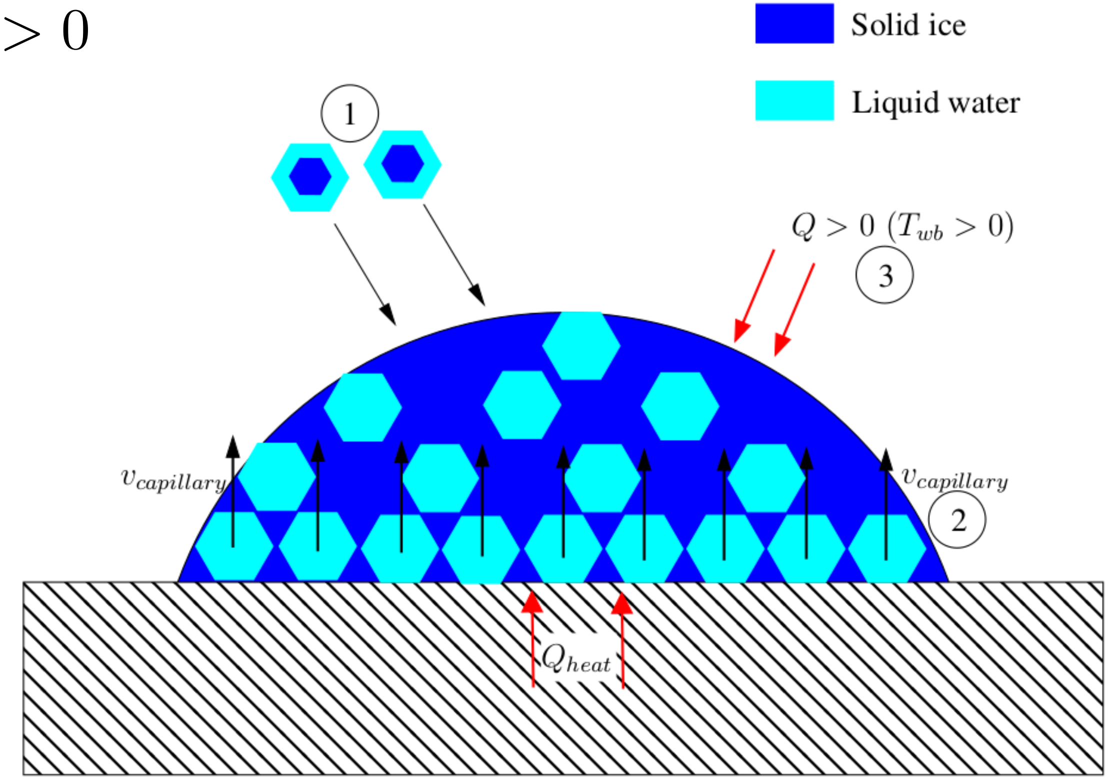

Sticking efficiency for ice crystal : definition of the wet bulb temperature

Wet bulb temperature T_{wb} :

- Temperature above a liquid film.
- Equilibrium temperature between evaporative cooling $\dot{\Phi}_{ev}$ and heat transfer $\dot{\Phi}_{conv}$
- Depends on the **relative humidity** r_h

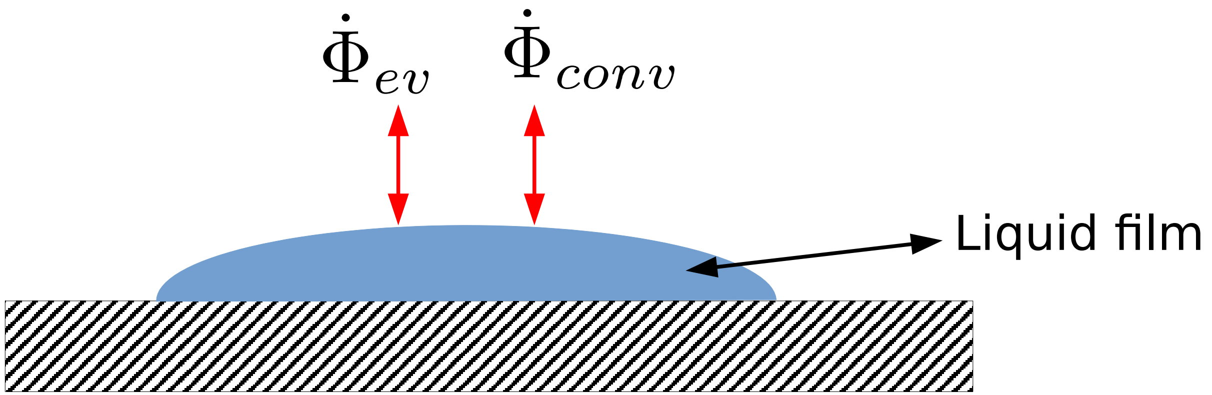

T_{wb} is solution of the non-linear equation :

$$\dot{m}_{ev}\left(T_{wb}\right) \cdot L_v(T_{wb}) = h_t \cdot \left(T_\infty - T_{wb}\right)$$

$\dot{m}_{ev}$: Evaporative mass

L_v : Latent heat of vaporization

h_t : Heat transfer coefficient

T_∞ : Farfield temperature

Sticking efficiency for ice crystal

For the **glaciated regime** (partially melted particles)

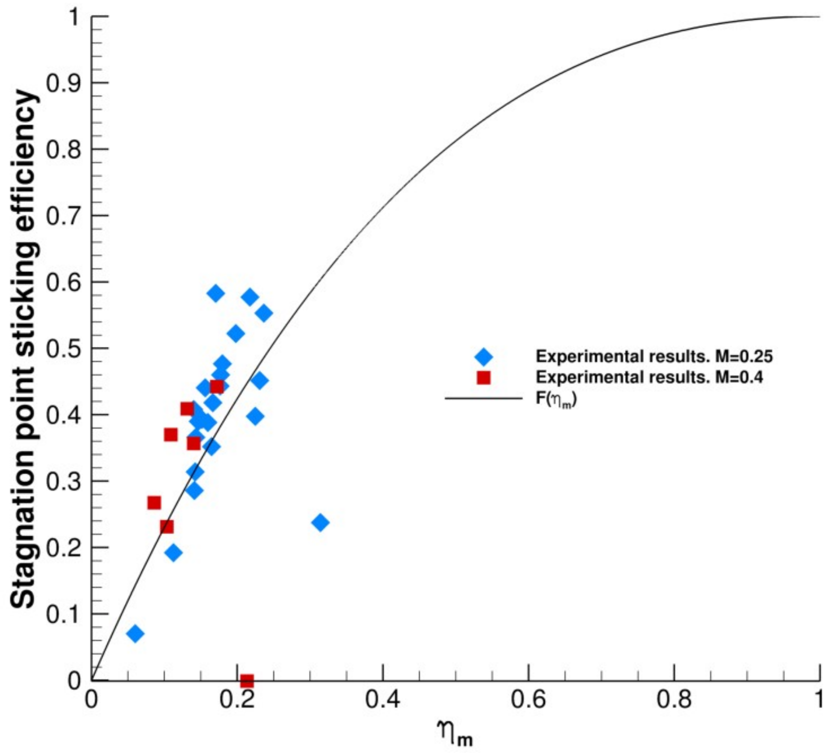

Currie, AIAA-2014-3049, 2014

$$\varepsilon_s = \frac{\dot{m}_{dep}}{\dot{m}_{imp}} = F(\eta_m)$$

η_m : particle melting ratio

- For the experiments, difficulty in differentiating between sticking efficiency and erosion which are **combined effects.**
- Measurements made near the stagnation point where erosion is observed as a minimum.

Characterization of the re-emitted particles: case of SLD

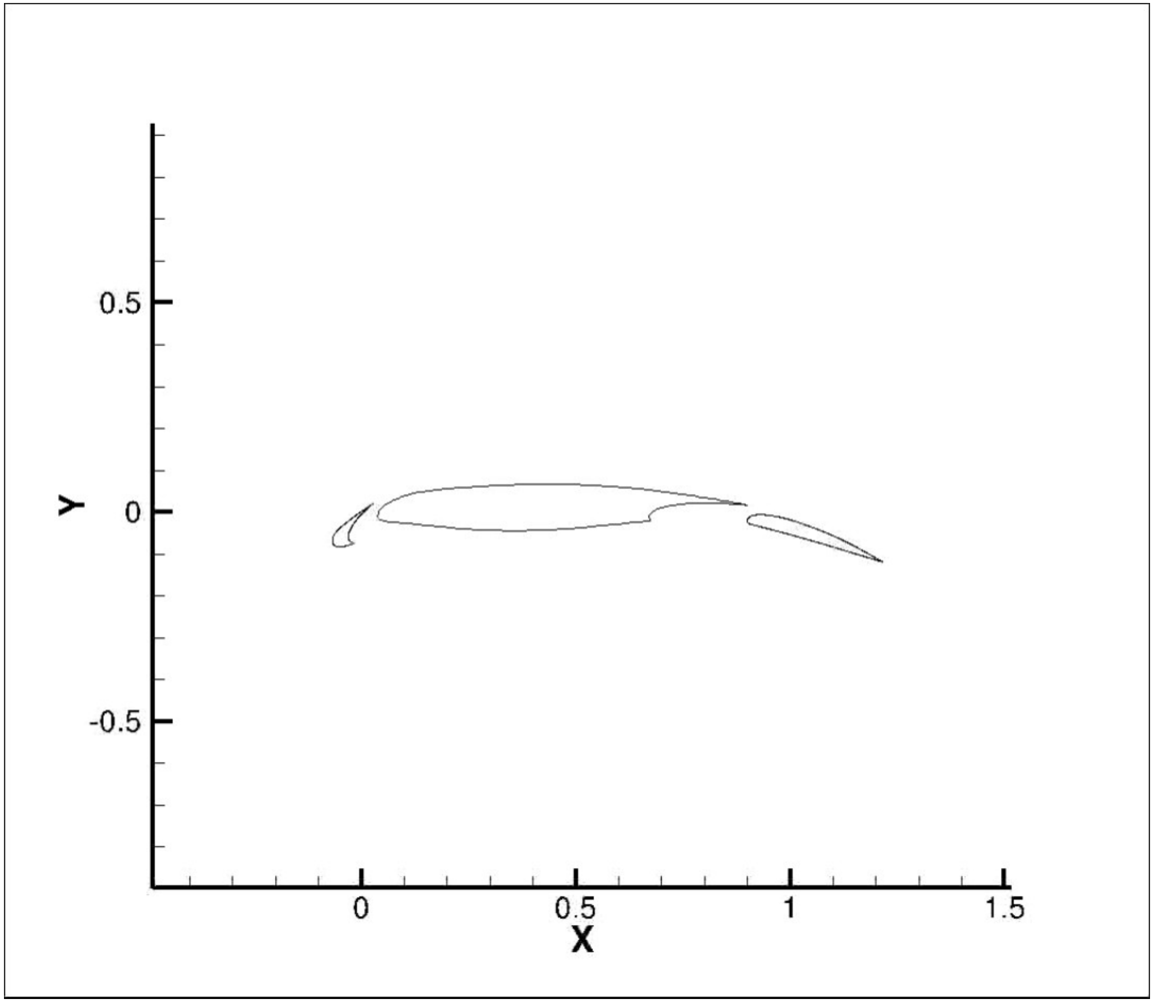

- **High-lift wing** with impacting SLD.

- Droplets re-emitted after impact on the slat can impact the main body and the flap **downstream**.

- Important for the **design of IPS** (Ice Protection System).

Characterization of the re-emitted particles: case of SLD

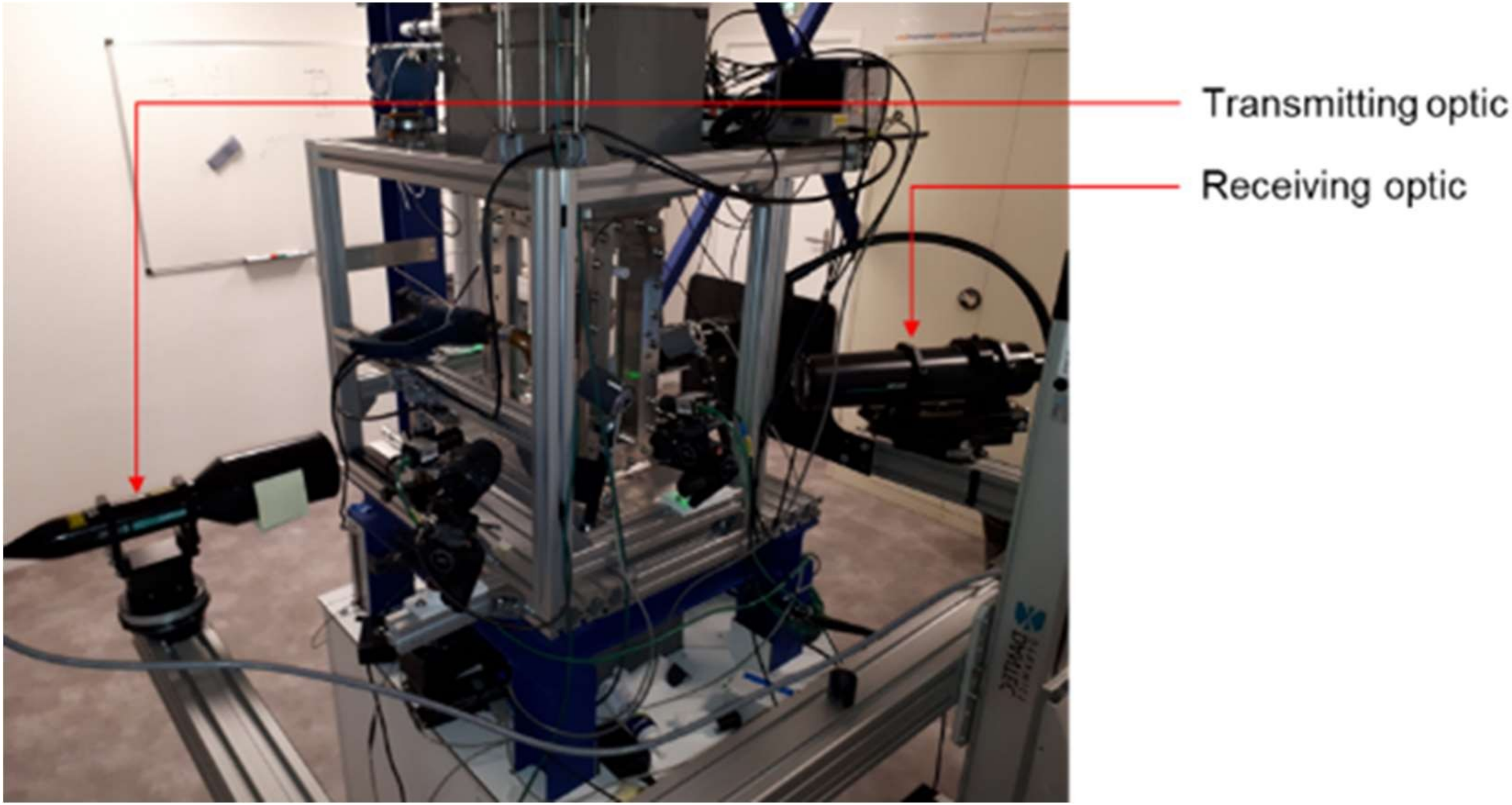

Experimental setup for secondary droplet diameter measurement with the Dantec DualPDA.
T. Alary PhD works (2023).

Characterization of the re-emitted particles: case of SLD

T. Alary PhD works (2023).

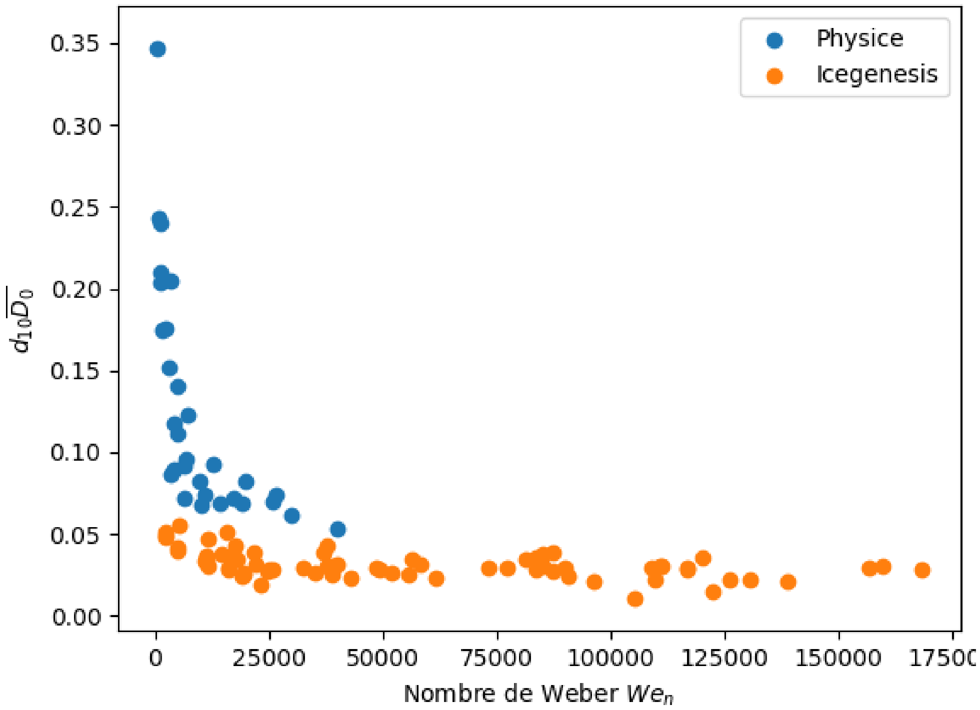

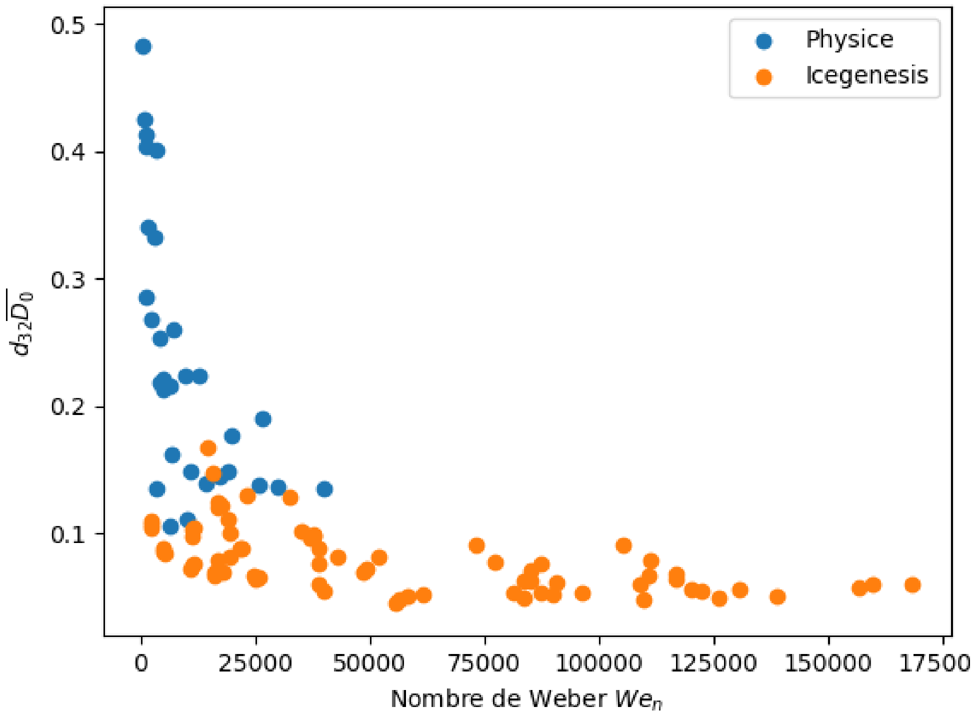

A **plateau** observed for the size of the re-emitted droplets for high velocities.

Characterization of the re-emitted particles: case of SLD

Smooth/clean surface

Iced surface

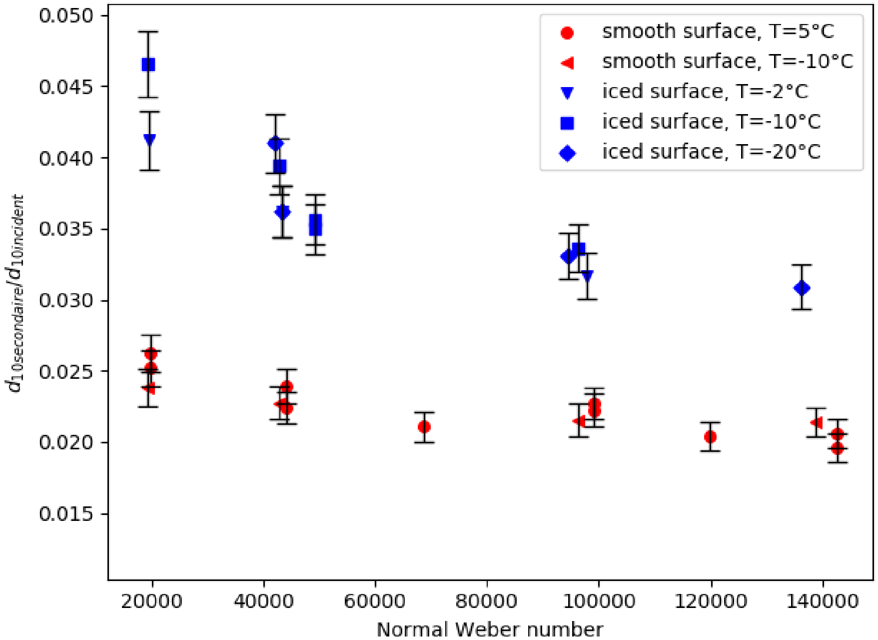

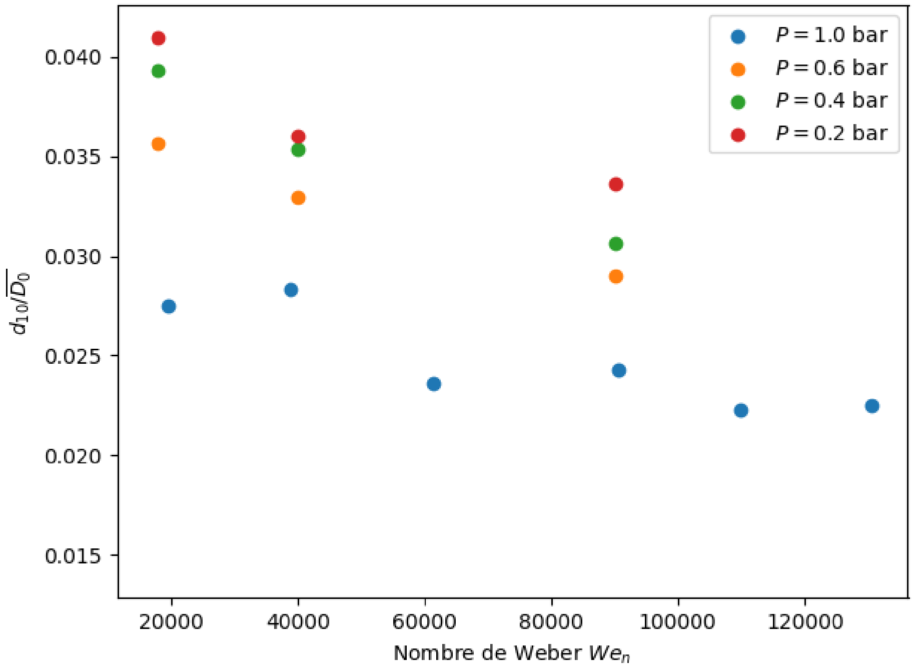

Influence of the substrate nature (iced vs. smooth/clean surface).

Pressure influence

Perspective : study of the ratio $\dfrac{d_{imp}}{h_{rough}}$

T. Alary PhD works (2023).

Characterization of the re-emitted particles: case of ice crystals. Estimation of the largest re-emitted fragment.

A Grady-based model (energy horizon model).

To predict the **maximum fragment diameter size**, two main impact stages are assumed:

- Crushing of the crystal within the wall contact zone and formation of an **indentation via plastic deformation**.
  (*Hutchings, J. Physics D, 1977, 10(14))*
  (Roisman and Tropea, Proc. R. Soc. A, 2015, 471)

- Due to the increasing tensile strain rate, whose level is determined by the indentation radius, cracks form to **relieve internal stresses**. The **energy horizon modeling framework of Grady for explosive fragmentation** is used to predict the largest fragment size.
  (*Grady, J. Mech. Phys. Solids, 1988, 36*)

Characterization of the re-emitted particles: case of ice crystals. Estimation of the largest re-emitted fragment.

Impact model: illustrations

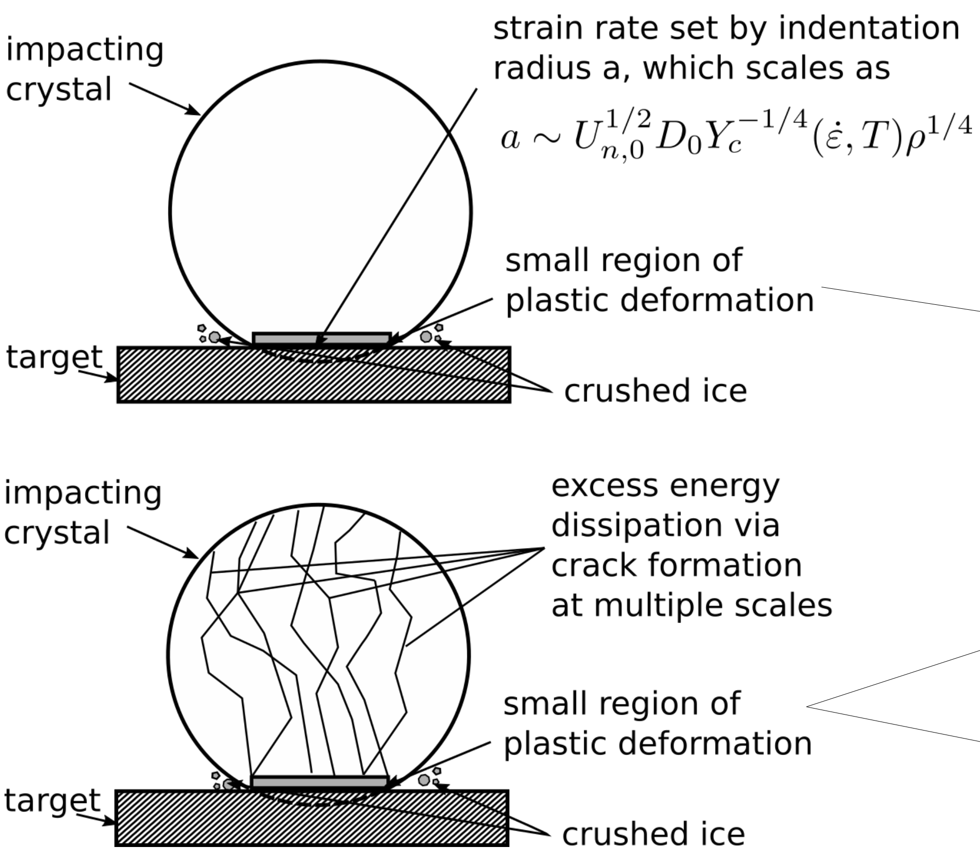

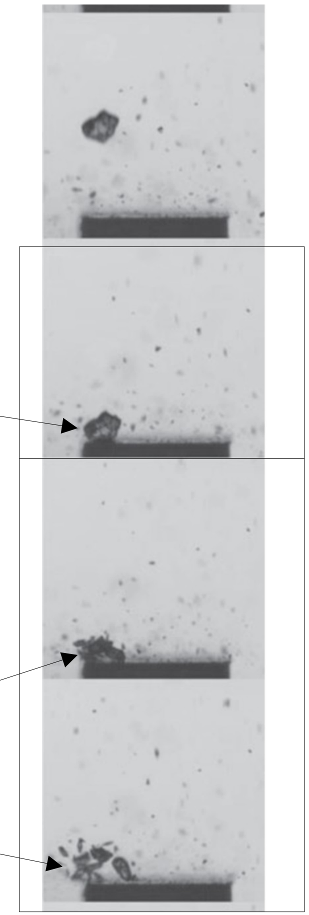

Schematic of the two main impact stages :
a) indentation formation via plastic deformation.
b) crack formation and fragmentation

Non spherical crystal impact visualization from Hauk et al.
(Hauk et al., Proc. R. Soc. A, 2015)

Maximum diameter model: details

- The strain rate is assumed to be related to the identation radius:

$$a \sim U_{n,0}^{1/2} D_0 Y_c^{-1/4}(\dot{\varepsilon}, T)\rho^{1/4}$$
$$\dot{\varepsilon} \sim U_{n,0}^{1/2} D_0^{-1} Y_c^{1/4}(\dot{\varepsilon}, T)\rho^{-1/4}$$

- with Y_c the compressive failure strength, which depends both on temperature (*Petrovic, J. Mat. Science, 2003*) and the strain rate itself (*Tippmann et al, Int. J. Imp. Eng., 2013*). The ice density ρ is assumed constant.

- Energy limited fragmentation is assumed, i.e. fragmentation through a sufficient inherent flaw structure when sufficient energy is supplied (*Grady, J. Mech. Phys. Solids, 1988, 36*):

$$\frac{D_{max}}{s_0} \sim \left(\frac{\dot{\varepsilon}}{\dot{\varepsilon}_0}\right)^{\beta}$$

Grady's energy-based model for the estimation of the largest fragment size

- An **energy-based** criterium for fragment size.
- Less attention attributed to the underlying microstructure involved in the fracture process.
- d : **fragment characteristic size**

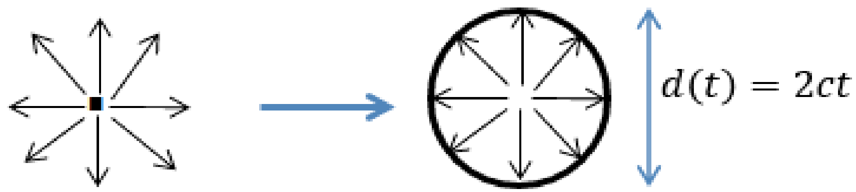

T=0s T=t

- Three energy contributions (in the particle frame):
  - Tensile (dilatation) energy : $E_{el} = \frac{\pi}{12}\varepsilon(t)\sigma(t)d(t)^3 = \frac{\pi}{12}\frac{\sigma(t)^2}{E}d(t)^3 = \frac{\pi}{12}\frac{\sigma(t)^2}{\rho c^2}d(t)^3$
  - Surface creation energy : $E_{surf} = \pi\Gamma d(t)^2$
  - Kinetic energy (neglected in comparison to the other contributions in the balance)
- Energy balance: $\boxed{\frac{1}{2}\frac{\sigma(t)^2}{\rho c^2} = \frac{6\Gamma}{d(t)}}$ (per volume unit)

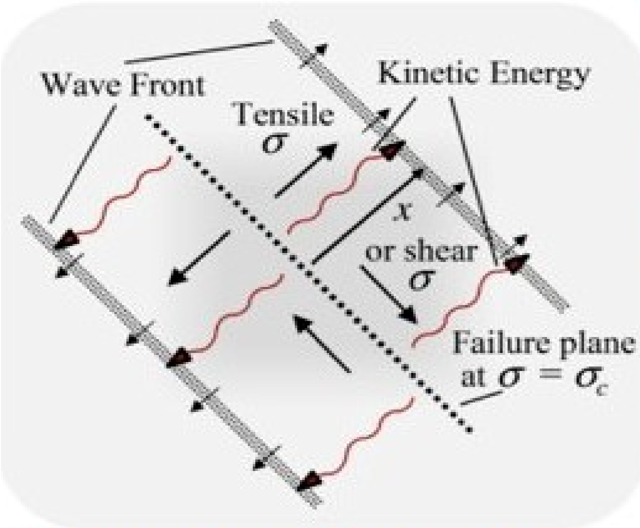

Material failure on the x = 0 plane initiates stress release wave propagation into the neighboring elastic medium

- ρ : density
- E : Young modulus
- $c^2 = \frac{E}{\rho}$: wave speed
- Γ : surface tension coefficient
- σ : tensile stress
- ε : strain
- Hooke law: $\sigma = E\varepsilon$

Grady's energy-based model for the estimation of the largest fragment size

Hypothesis:

- $d(t) = 2ct$
- $\sigma(t) = \rho c^2 \dot{\varepsilon} t$
- $\dot{\varepsilon}$ **(strain rate)** large enough so that $t_1 < t_2$ (energy-limited fragmentation mode in the energy-horizon theory of Grady)
- Y : yield strength (maximum tensile pressure)

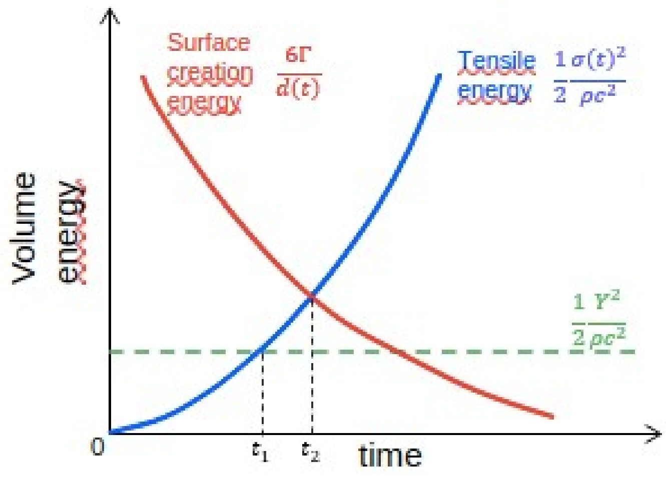

Static approach:

- For $t \geq t_1$: fragmentation with $\sigma(t) = \sigma_1 = Y$ and $\frac{1}{2}\frac{\sigma(t)^2}{\rho c^2} = \frac{1}{2}\frac{Y^2}{\rho c^2}$

$$\rho c^2 \dot{\varepsilon} t_1 = Y$$

- $t_1 = \frac{d_1}{2c}$

$$\dot{\varepsilon} d_1 = \frac{2Y}{\rho c}$$

$$\boxed{\frac{\dot{\varepsilon}}{\dot{\varepsilon}_*}\frac{d_1}{d_*} = 1}$$

Dynamic approach (energy-horizon theory):

- For $t = t_2$: $\frac{1}{2}\frac{\sigma_2{}^2}{\rho c^2} = \frac{6\Gamma}{d_2}$

$$\rho c^2 \dot{\varepsilon}^2 t_2 = \frac{12\Gamma}{d_2}$$

- $t_2 = \frac{d_2}{2c}$

$$\dot{\varepsilon}^2 d_2{}^3 = \frac{48\Gamma}{\rho}$$

$$\boxed{d_* = \frac{12\rho c^2 \Gamma}{Y^2} \qquad \dot{\varepsilon}_* = \frac{Y^3}{6\rho^2 c^3 \Gamma}}$$

$$\boxed{\left(\frac{\dot{\varepsilon}}{\dot{\varepsilon}_*}\right)^2 \left(\frac{d_2}{d_*}\right)^3 = 1}$$

Grady's energy-based model for the estimation of the largest fragment size

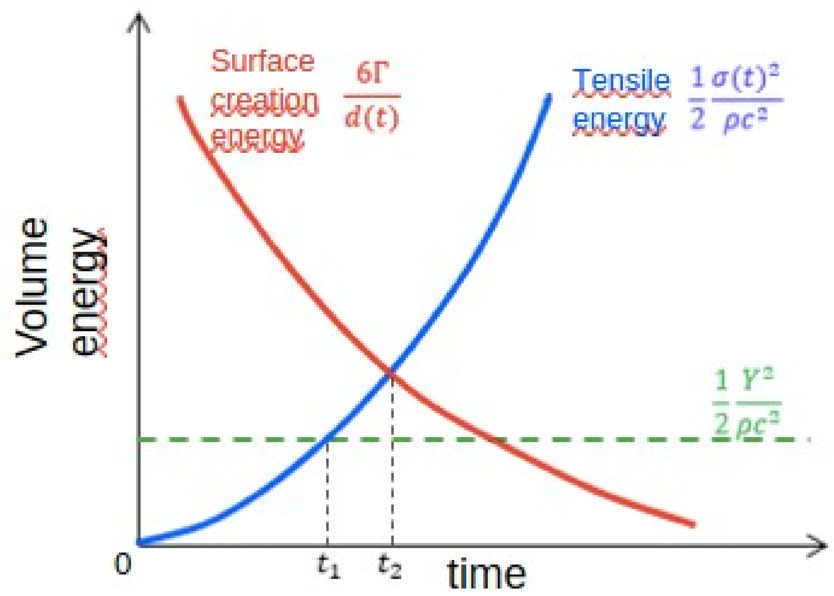

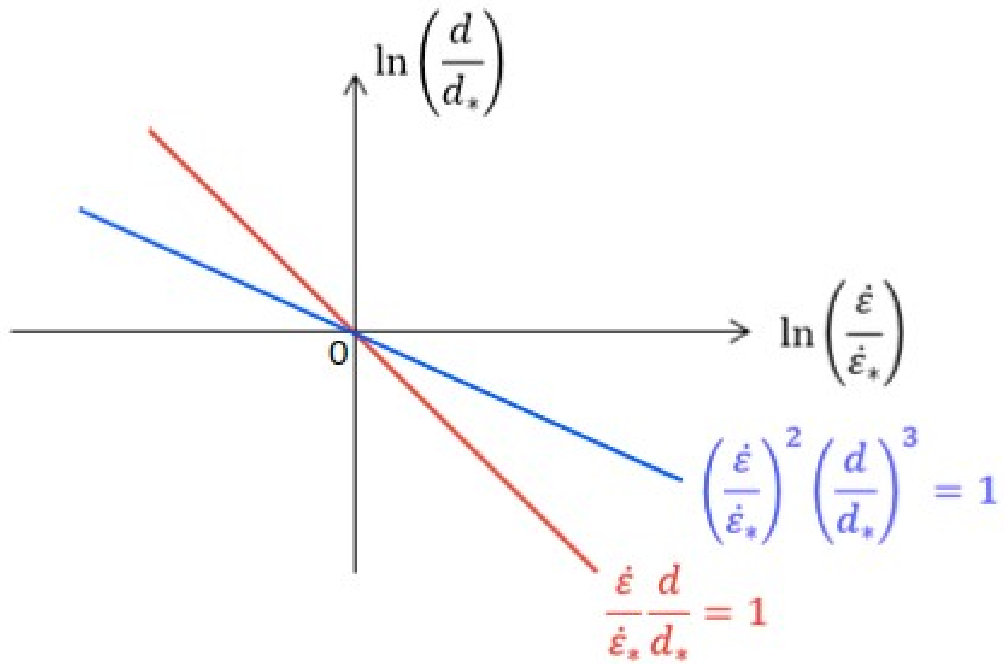

$t_1 < t_2$ ➔ d provided by the dynamic approach
$t_1 > t_2$ ➔ d provided by the static approach

Limit: $t_1 = t_2$ ➔ $t_1 = t_2$ ➔ $\boxed{d_{lim} = d_* \approx 150 \mu m}$

E = 10.5 GPa
Y = 10 MPa
Γ = 0.12 J/m^2
ρ_p = 917 kg/m^3

In conclusion:

- Determine α and β such that $\frac{d}{d_*} = \alpha\left(\frac{\dot{\varepsilon}}{\dot{\varepsilon}_*}\right)^{-\beta}$ with $1 \leq \beta \leq 2/3$

Maximum diameter model: details

$$\frac{D_{max}}{s_0} \sim \left(\frac{\dot{\varepsilon}}{\dot{\varepsilon}_0}\right)^{\beta}$$

The exponent should lie **between -1 (static fracture) and -2/3 (highly dynamic fracture)**, so a slightly lower (absolute value) exponent value was expected

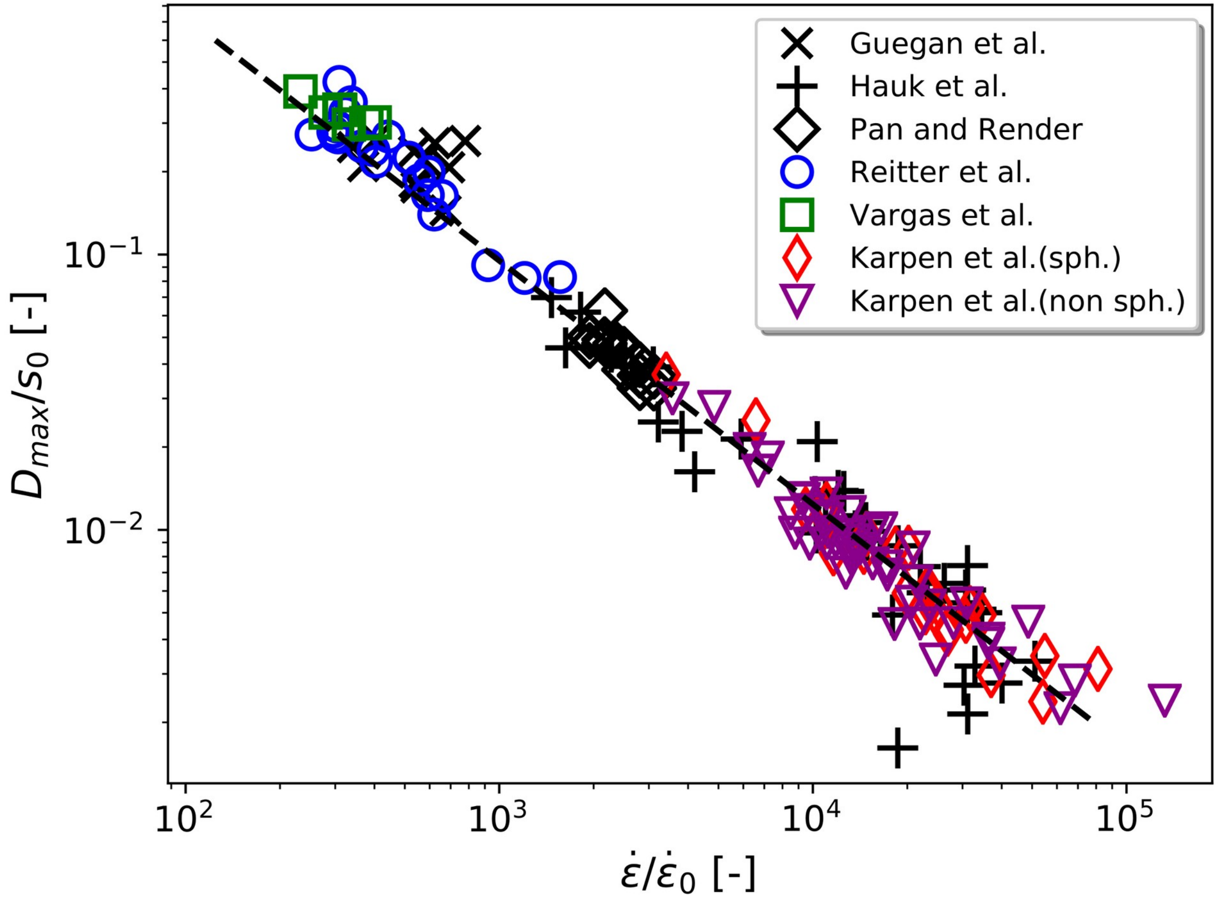

Senoner *et al.*, IJIE, 2022

Correlation between current strain rate model and maximum particle diameter in a log-log plot.

Particle size distribution (PSD)

- Weiss (Weiss, *Eng. Fract. Mech., 68 (17-18)*) assumes that the size distribution resulting from ice crystal impact is **fractal in nature**, i.e. number probability density for instance follows a power law:

$$p(x)dx = Pr\left(x \leq X \leq x + dx\right) = Cx^{-\alpha}dx$$

- The main idea of fractals applied to fragmentation is that t**he rupture propagates from the largest to the smallest scales** with an identical rupture criterion, mostly the same rupture probability at all scales.

- Grady proposes an **loose analogy** with turbulence for understanding: “during failure, fracture on successively finer length scales proceeds though a cascade of crack branching until length scales adequate to the dissipation of the initial elastic strain energy are achieved”.

Particle size distribution (PSD)

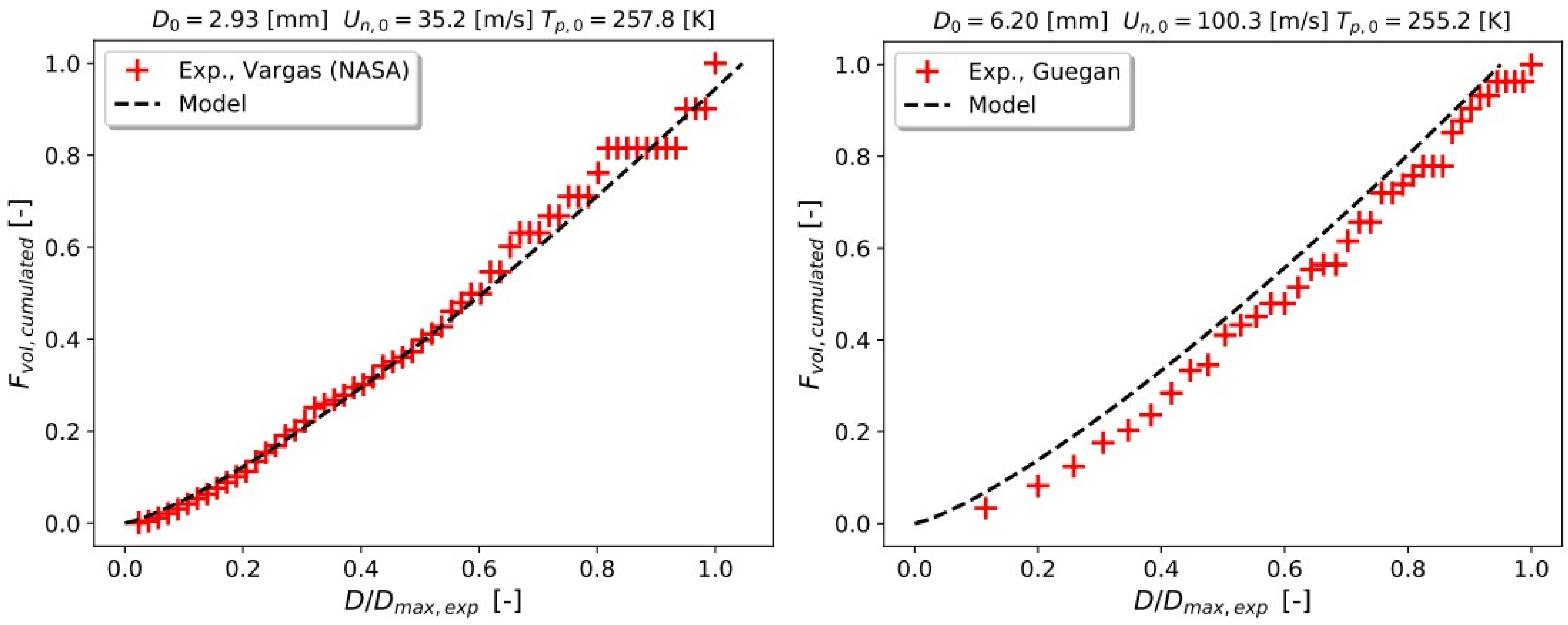

Senoner *et al.*, IJIE, 2022

$F_{vol,cumulated}$: cumulative particle size distribution

Particle velocity distribution

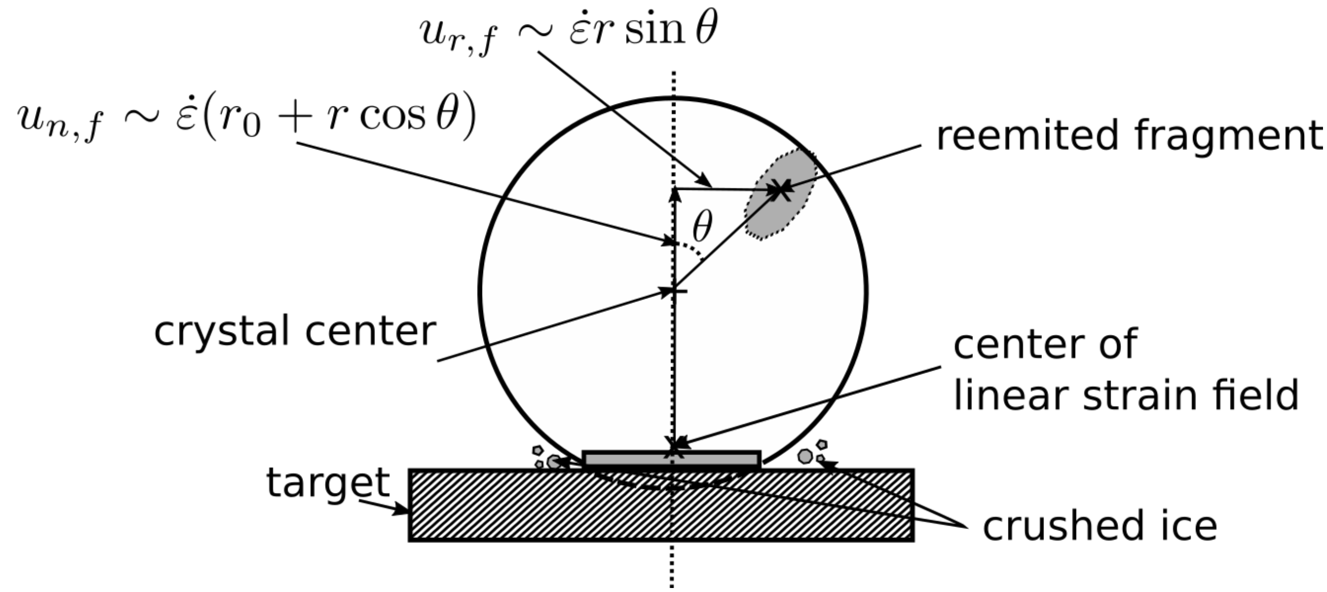

Schematic of the fragment velocity model assuming a linear strain rate distribution centered on the lower bottom of the crystal

The number averaged radial and normal velocities then write :

$$\overline{u_{f,r}} = \int_{r_{min}}^{r_{max}} C r_f^{-\alpha} \int_0^{r_0-r_f} \int_0^{2\pi} \int_0^{2\pi} \frac{1}{4/3\pi(r_0-r_f)^3} k\dot{\varepsilon} r \sin\theta r^2 \sin\theta \, d\phi \, d\theta \, dr \, dr_f$$

$$\overline{u_{f,n}} = \int_{r_{min}}^{r_{max}} C r_f^{-\alpha} \int_0^{r_0-r_f} \int_0^{2\pi} \int_0^{2\pi} \frac{1}{4/3\pi(r_0-r_f)^3} k\dot{\varepsilon}(r_0 + r\cos\theta) r^2 \sin\theta \, d\phi \, d\theta \, dr \, dr_f$$

Senoner *et al.*, MUSIC-haic, 2022

Characterization of the re-emitted particles: case of ice crystals. Particle velocity distribution.

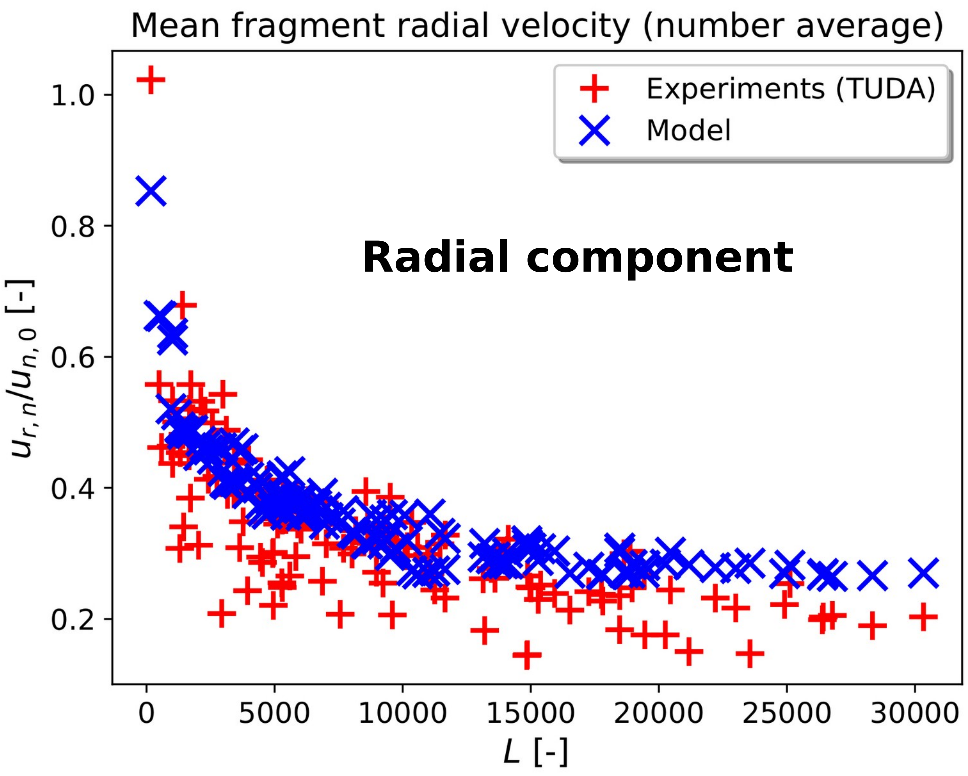

Ratio of number averaged radial fragment velocity over the Vidaurre number L

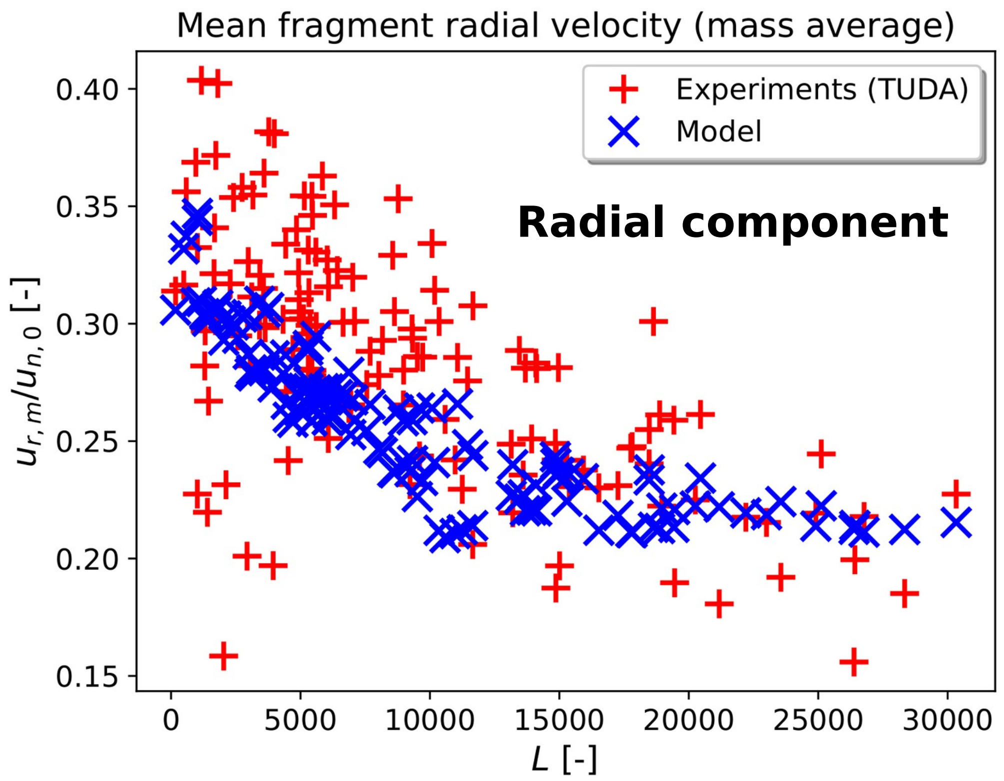

Ratio of mass averaged radial fragment velocity over the Vidaurre number L

Normal component

$$\overline{u_{f,n}} = \frac{k'}{2} u_n^{1/2} Y_c^{1/4} \rho^{-1/4}$$

For the n**ormal velocity**, the average restitution coefficient **does not depend on the size of the impacting crystal and is constant regardless of the size of the reemited fragments**, which **does not seem realistic.**

➡ Additional work required for the normal component.

Senoner *et al.*, MUSIC-haic, 2022

Outline

1) Trajectory model adaptation for SLD, ice crystals and snowflakes.

2) Impact model adaptation for SLD, ice crystals and snowflakes.
   a) SLD
   b) Ice crystals

3) Accretion model adaptation for SLD, ice crystals and snowflakes.

The plateau effect (ice crystal icing, glaciated conditions).

Currie *et al.*, AIAA 2014

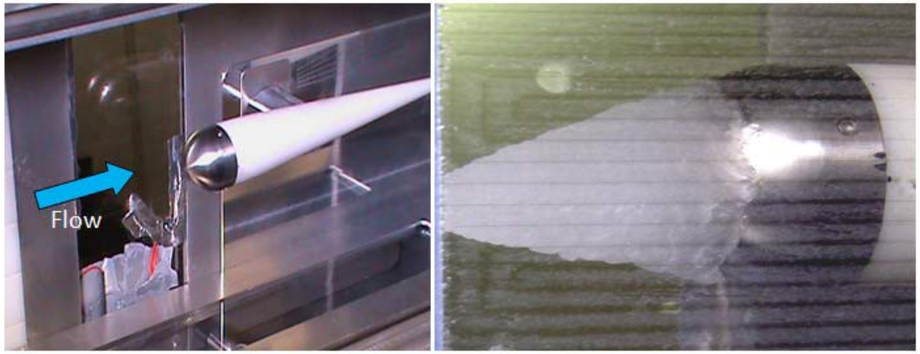

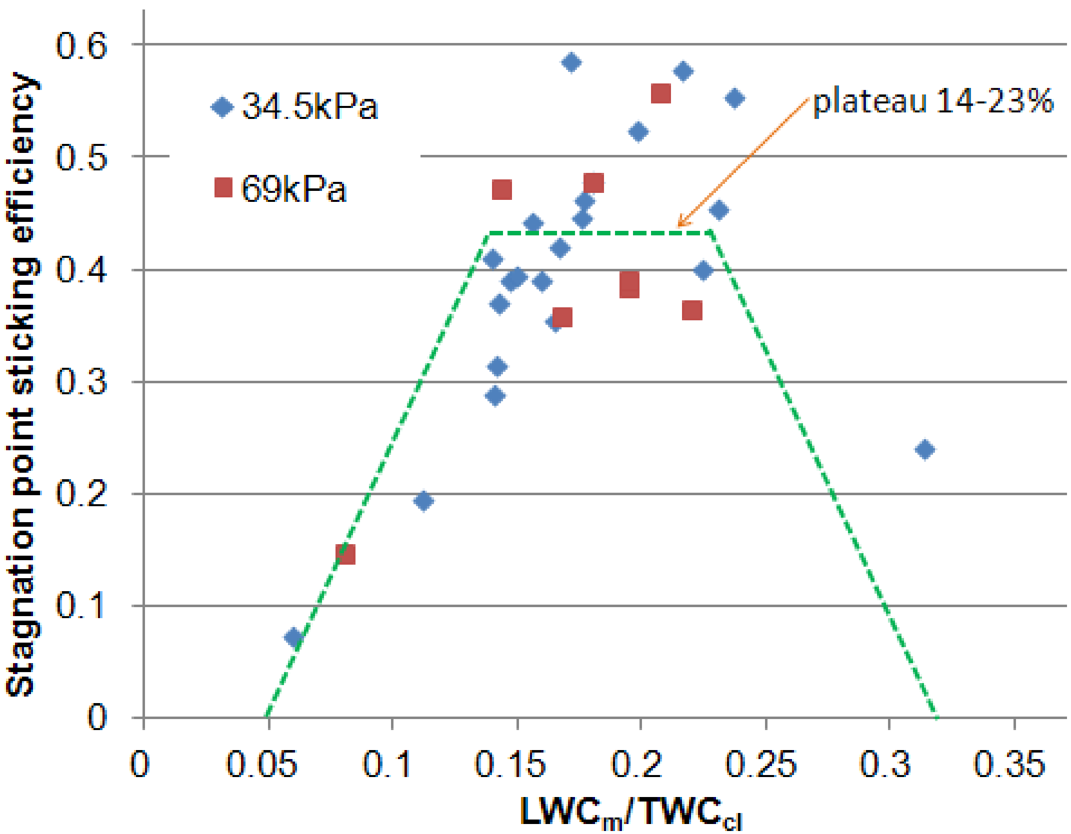

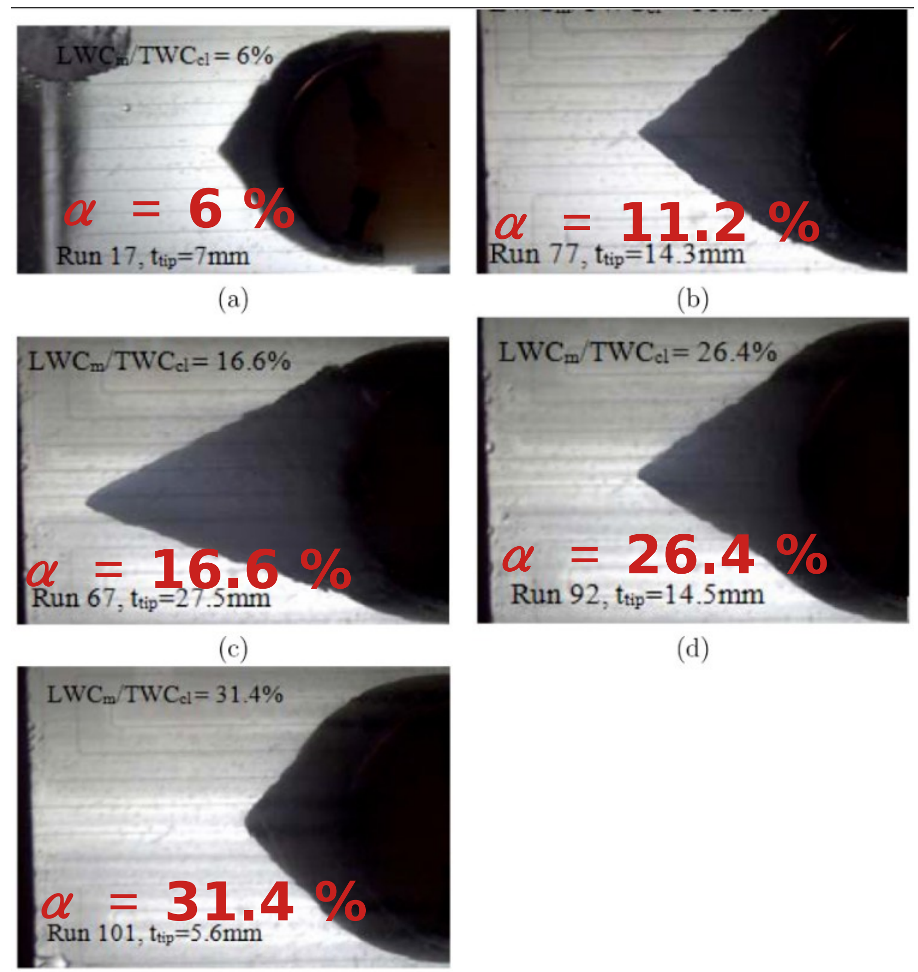

The plateau effect (ice crystal icing, glaciated conditions).

- **Competition** between the particle **sticking efficiency and erosion**.
- Relevance of the role played played by the **liquid water**.

Low melting ratio η_m:
- Increasing sticking efficiency ε_s with melting ratio.
- Moderate erosion (few water)

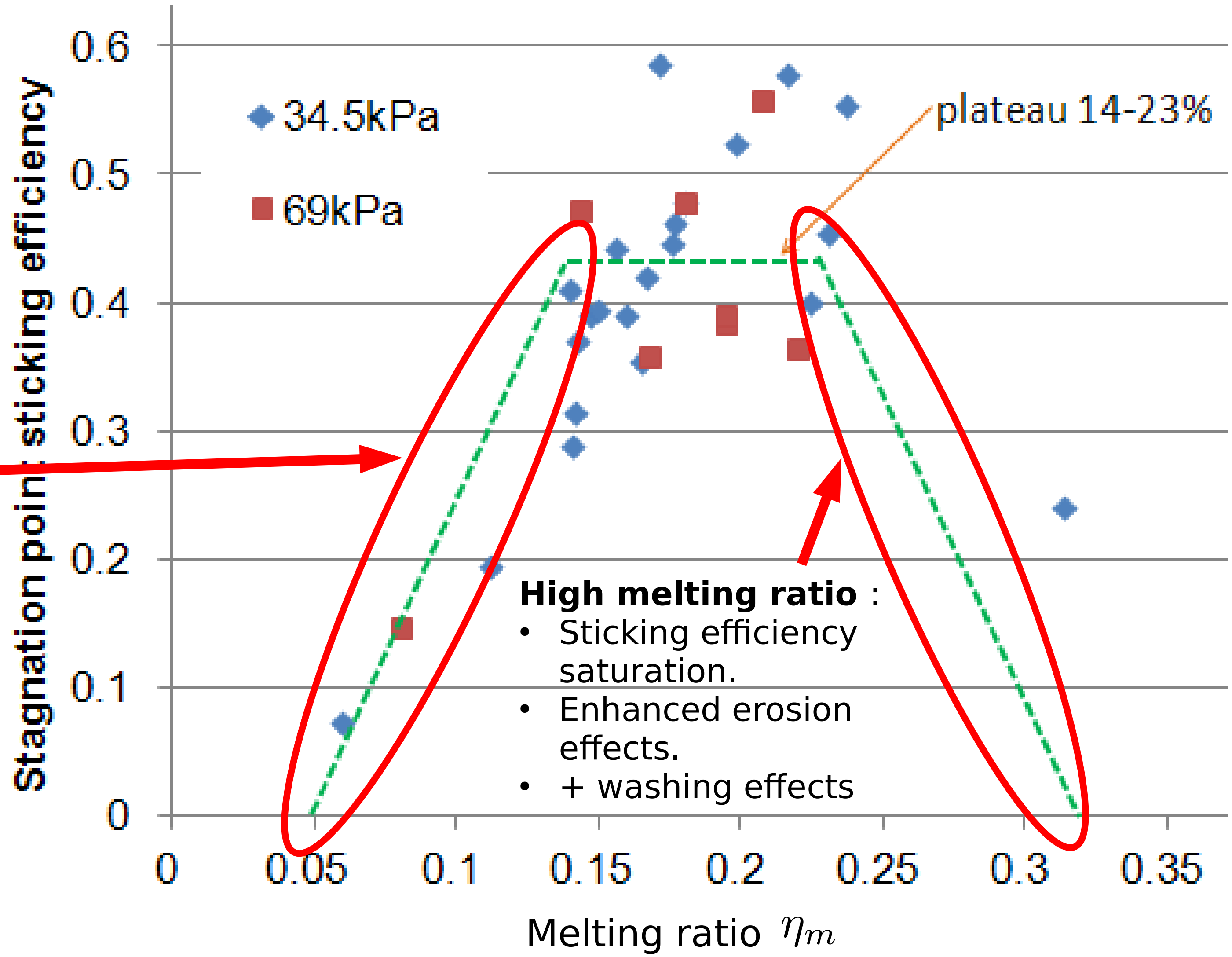

High melting ratio :
- Sticking efficiency saturation.
- Enhanced erosion effects.
- + washing effects

Currie *et al.*, AIAA 2014

Consideration of the erosion effect : ice shapes in ice crystal icing conditions

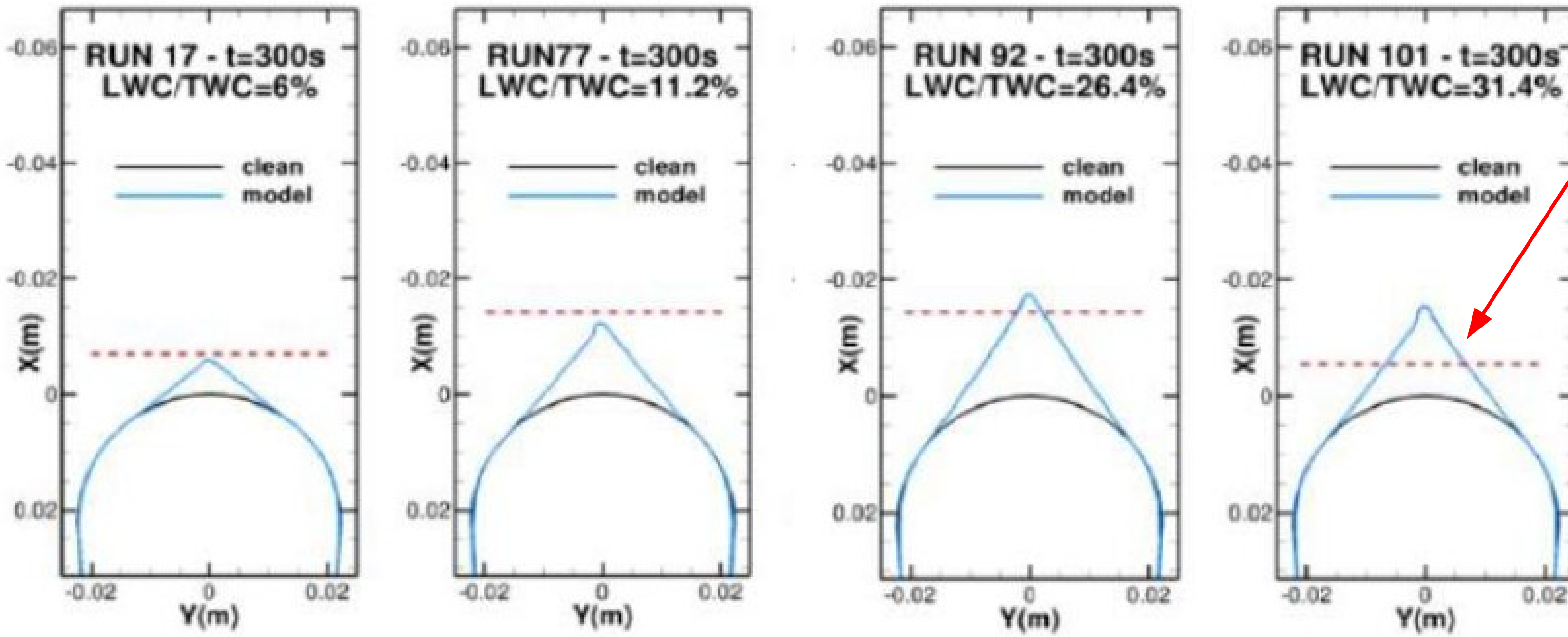

Only the tangential component of the velocity is considered

⇒ **Poor estimation** of the right part of the plateau.

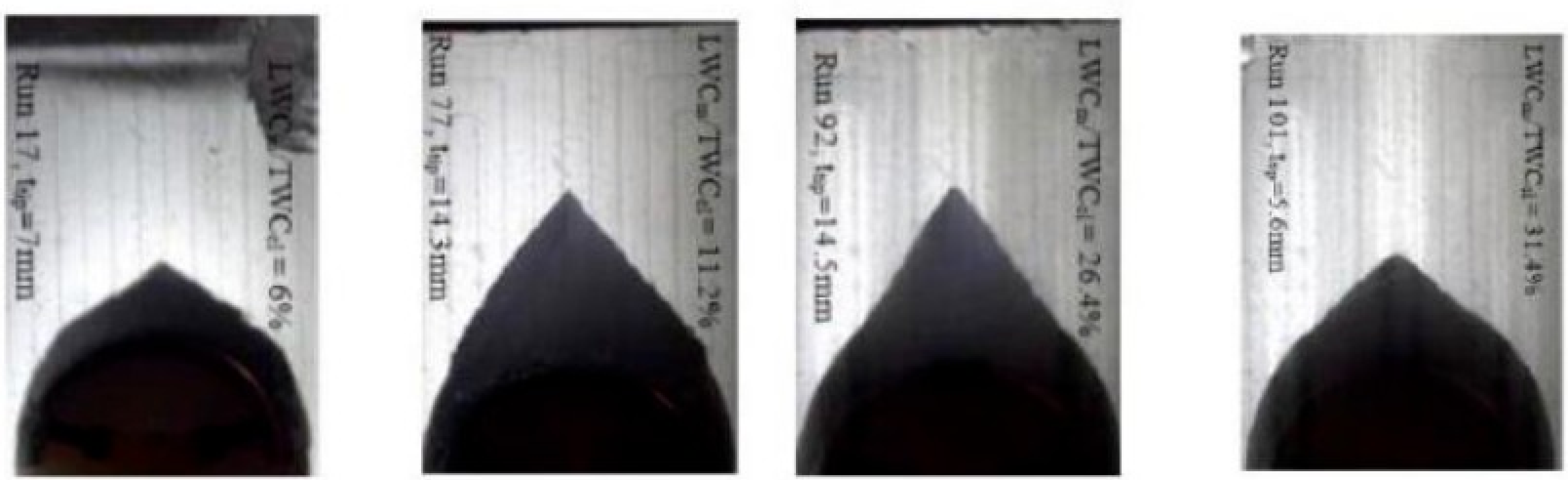

Erosion effect due to ice crystal impacts : model improvement (1/2)

- **Solid-solid collision theory** of Finnie et Bitter *[Finnie 1978, Bitter 1962]*
- Two main phenomena: plastic deformation and cutting.

Erosion by plastic deformation

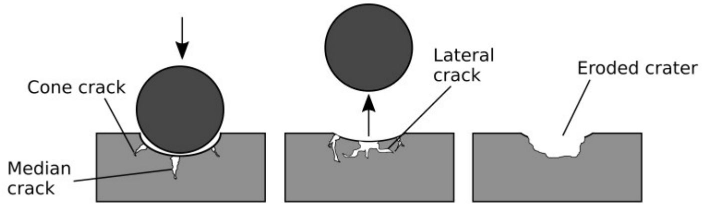

- Cratering by plastic deformation
- Large influence of the normal velocity.

Erosion by cutting

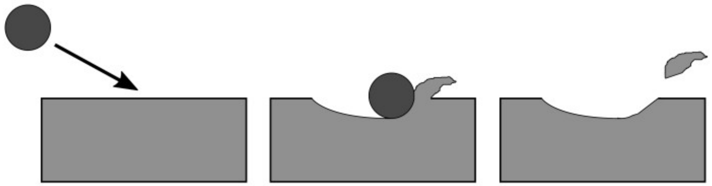

- A part of the substrate is torn off after penetration of the particle.
- Large influence of the tangential velocity

$$\eta_{er}=\frac{m_{er}}{m_{imp}}=F_s\rho\frac{\boldsymbol{V_c}(v_t^2,C,\sigma_{el})+\boldsymbol{V_d}(v_n^2,E,\nu,\sigma_{el},\varepsilon_D)}{m_{imp}}$$

F_S : shape factor
σ_{el} : yield strength
E : Young modulus
ν : Poisson coefficient
ε_D : deformation wear factor
C : cutting efficiency

Erosion effect due to ice crystal impacts : model improvement (2/2)

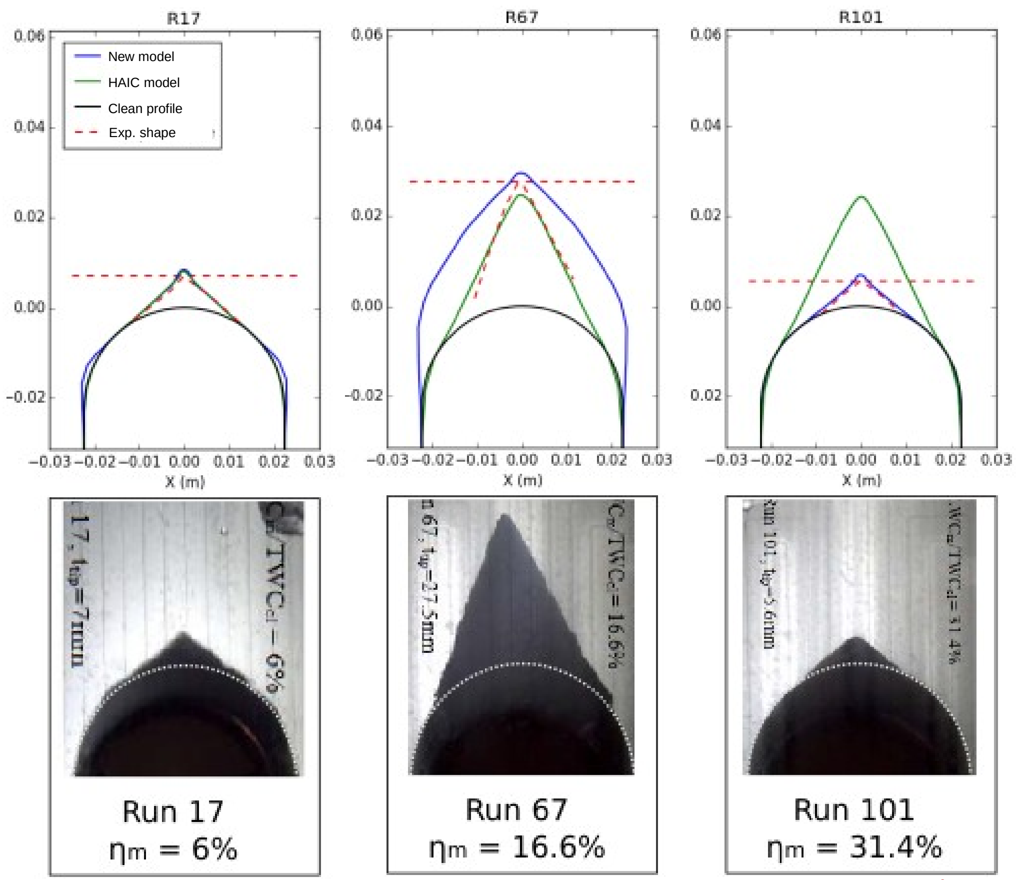

$\eta_m \nearrow$

$\eta_m \nearrow$ ➡ Liquid fraction in the ice layer $\nearrow$

➡ $\sigma_{el} \searrow$ $E \searrow$

➡ Better estimation of the right part of the plateau

Impact of solid ice particles on heated walls